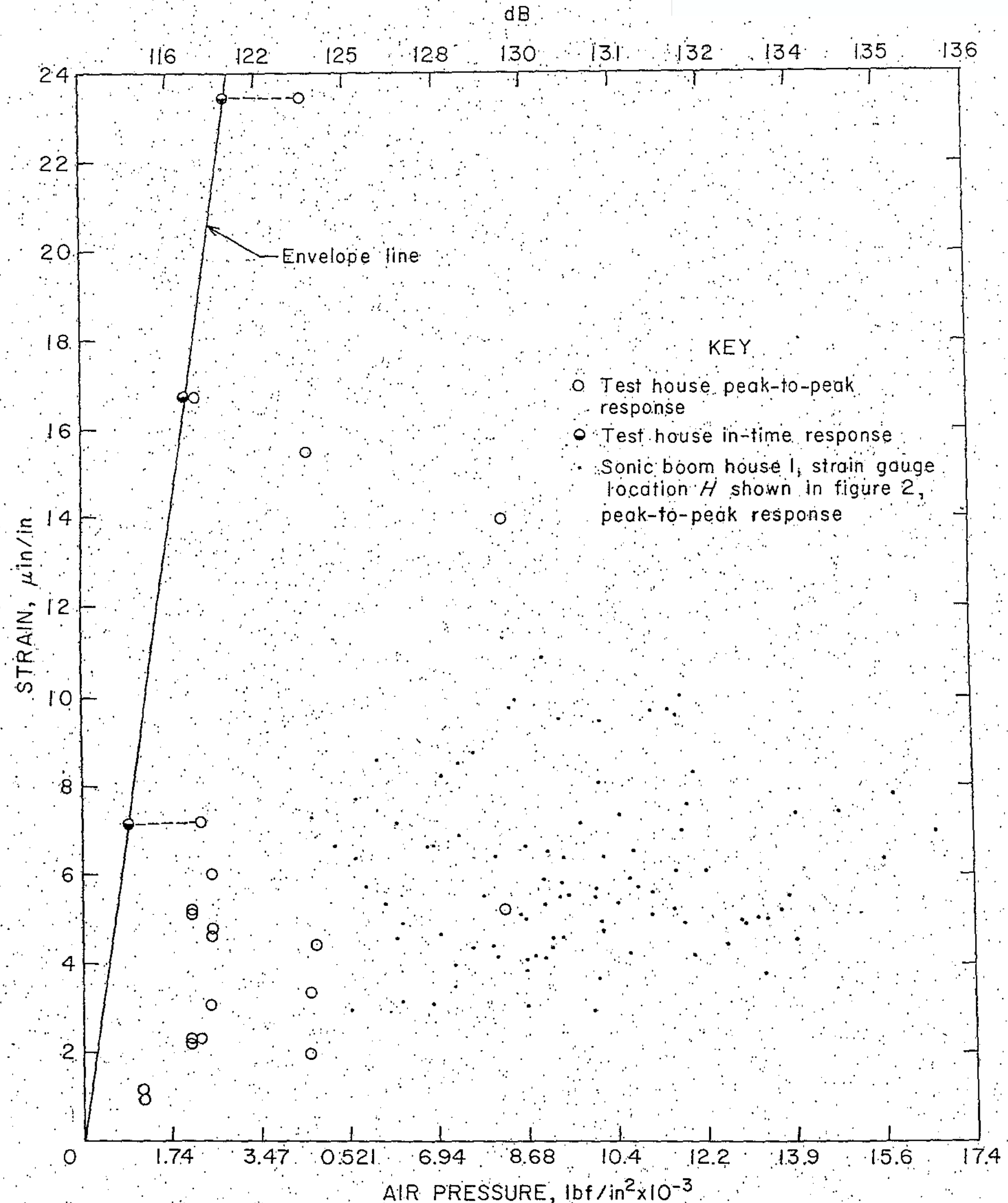

FIGURE 31. - Wallboard strain versus airblast level at test house, with comparison to sonic boom response.

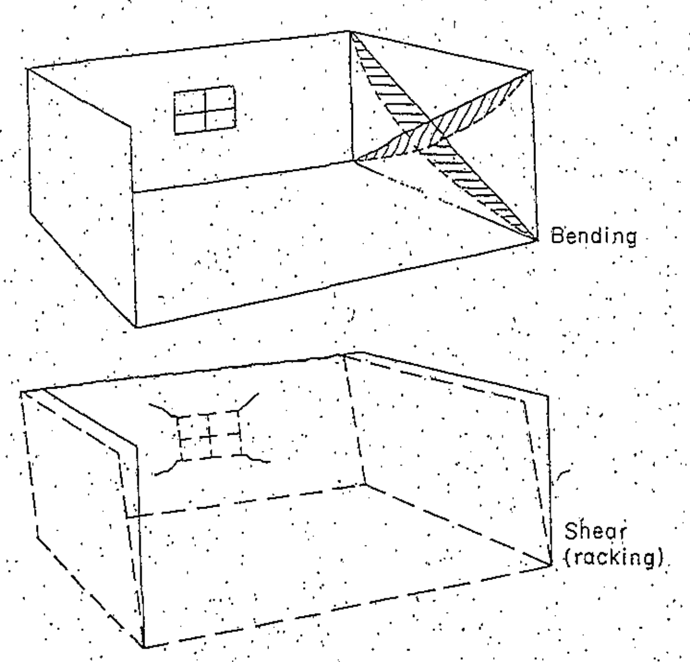

FIGURE 32. - Shear and flexure response of walls (2).

Table 10 displays the shaker sweep and fatigue data in the order in which the tests were run. The house's response to sweeps 1 and 2 provided initial frequency and amplitude data which were used to estimate shaker force settings and confirm the type of superstructure and foundation excitation. Equivalent ground motions are also given in table 10; for each run, one equivalent is based on the response at A_4 (high corner, east wall), and the other on the response at K_2 (fig. 13). Based on the responses to the first 40 shots, a ground vibration amplification factor of 3 was employed (i.e., if a 0.5-in/s ground vibration equivalency was desired, the output at A_4, high corner, east wall, had to be 1.5 in/s). At frequencies other than resonance, the amplification factor would be less than 3.

TABLE 10. - Mechanical shaker program description

Test	Ground vibration equivalency,[1] in/s		Number of shakers	Mode excited	Resonance frequency, Hz	Damping, pct	Acceleration, G		Cycles achieved
	A_4	K_2					At north gauge	At south gauge	
Sweep 1.	NAp	NAp	2	Translation	7.40	11.2	NA	0.15	8,000
Sweep 2.	NAp	NAp	2	Torsion....	9.35	5.9	NA	.36	8,000
Sweep 3.	NAp	NAp	2	Translation	7.20	10.5	NA	.28	8,000
Run 1...	0.44	0.61	2	...do......	7.20	NA	0.18	.26	100,192
Sweep 4.	NAp	NAp	2	...do......	6.95	11.0	NA	.26	8,000
Sweep 5.	NAp	NAp	2	Torsion....	8.65	NA	NA	.35	8,000
Run 2...	.55	.71	2	...do......	8.65	NA	.31	.35	100,171
Sweep 6.	NAp	NAp	2	...do......	8.30	NA	NA	.41	8,000
Sweep 7.	NAp	NAp	2	Translation	6.80	6.2	NA	.42	8,000
Run 3...	.30	.29	[2]1	Torsion....	7.00	NA	.12	.24	60,000
Sweep 8.	NAp	NAp	[2]1	...do......	6.65	NA	NA	.36	8,000
Sweep 9.	NAp	NAp	[2]1	...do......	6.45	NA	NA	.46	8,000
Run 4...	.73	.49	[2]1	...do......	6.45	NA	.21	.44	60,070
Sweep 10	NAp	NAp	[2]1	...do......	6.25	12.5	NA	.42	8,000
Sweep 11	NAp	NAp	[2]1	...do......	5.90	NA	NA	.58	8,000
Run 5...	1.1	.53	[2]1	...do......	5.90	NA	NA	.58	36,240

NA Not available. NAp Not applicable.

[1]Based on envelope line of strain (at site K_2 in figure 13) or structure motion (at site A_4 in figure 13; high corner, east wall) versus ground vibration data.

[2]At south end of test house only.

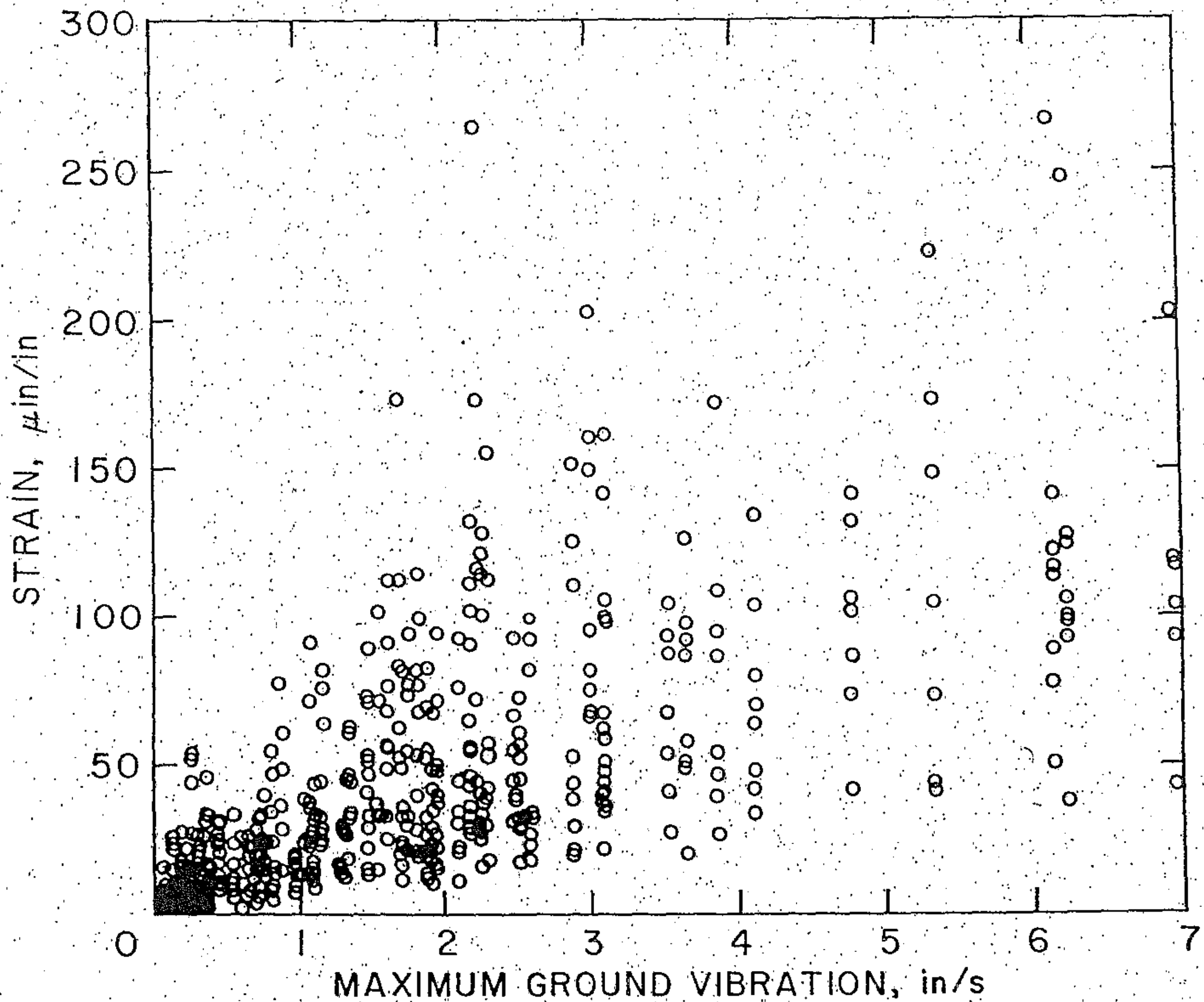

FIGURE 33. - Wallboard and plaster strain versus maximum ground vibration.

Later cyclic tests varied from the planned approach because the shaker at the north end of the house failed prior to run 3. The level of excitation was readjusted for response variances caused by one driving shaker. While the desired 0.50-in/s ground vibration equivalency was attained for runs 1 and 2, the eccentricity of the only operating shaker (southend) was not changed for subsequent runs, and the vibration equivalency dropped to ~ 0.30 in/s for run 3 (table 10). Runs 4 and 5 were also performed with only one shaker and hence produced predominately torsion. Thus, the responses at A_4, high corner, east wall, and K_2 were not similar since K_2 was located close to the instantaneous center of rotation.

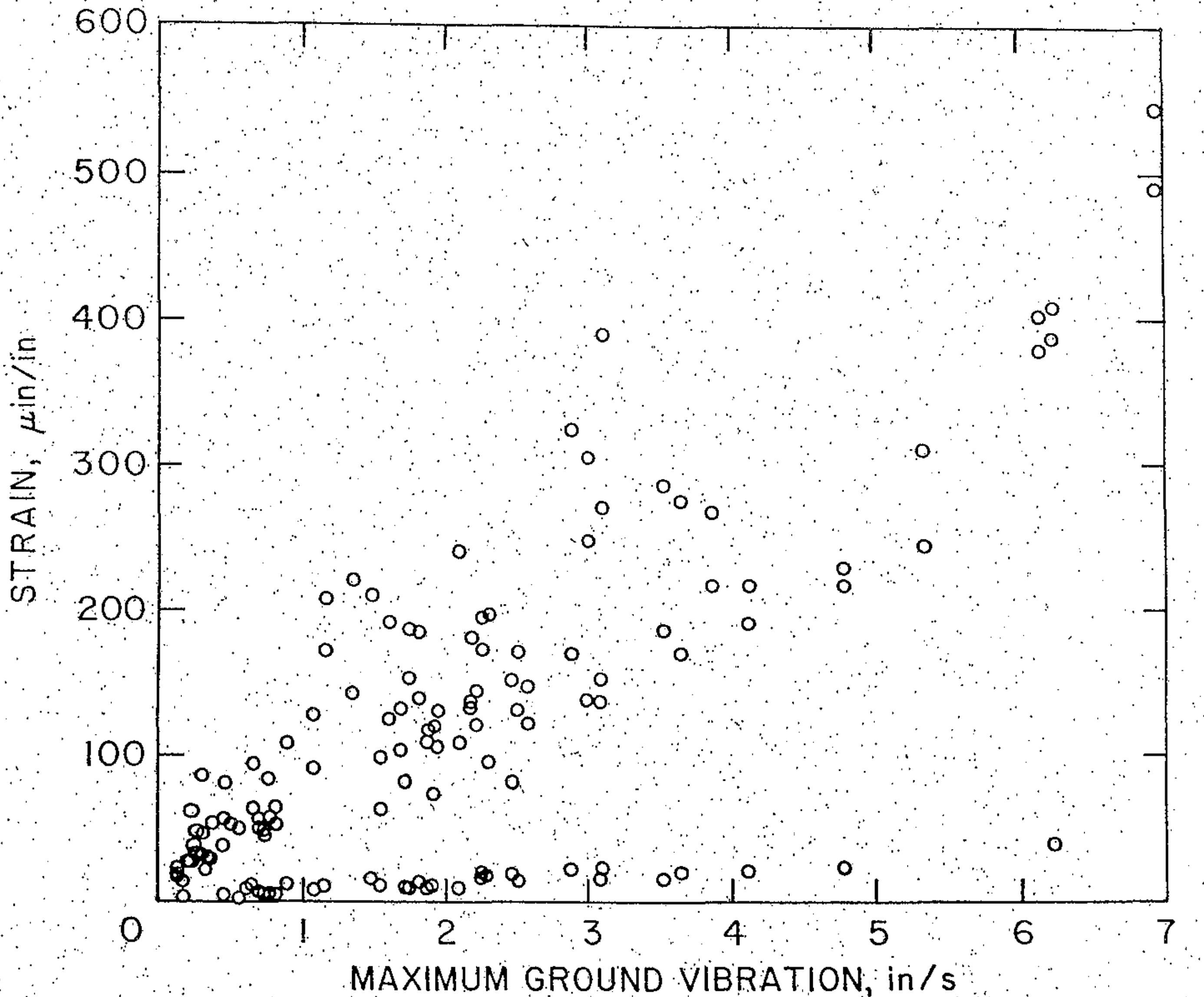

FIGURE 34. - Wallboard tape joint strain versus maximum ground vibration.

The superstructure decreased in stiffness, as shown by the drop in natural frequency plotted in figure 38. In addition, flexure was observed at the small areas of dimpled wallboard around nailheads; as previously indicated, the nailheads limited the transfer of energy to the strain-monitored sites.

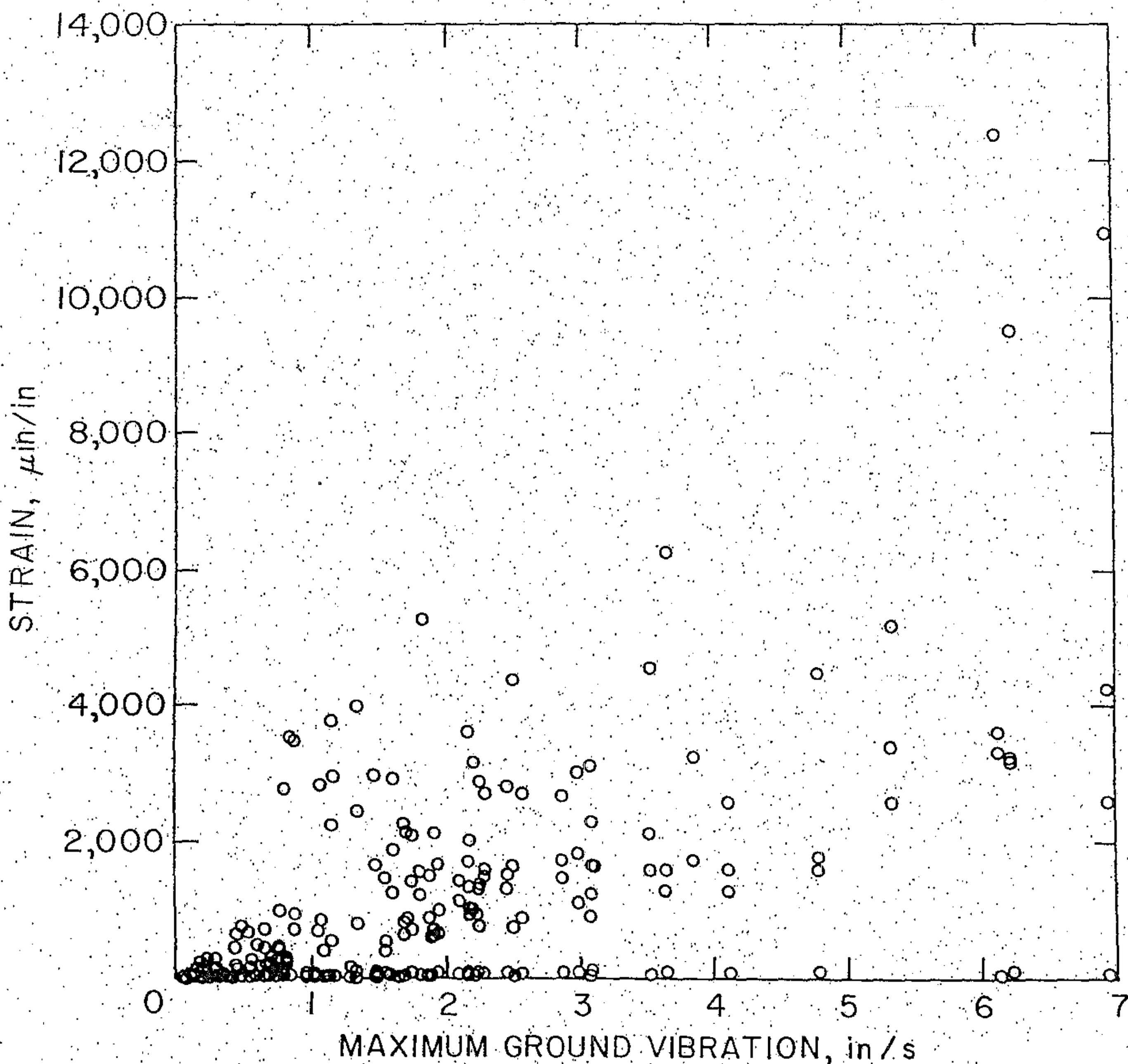

FIGURE 35. - Block joint strain versus maximum ground vibration.

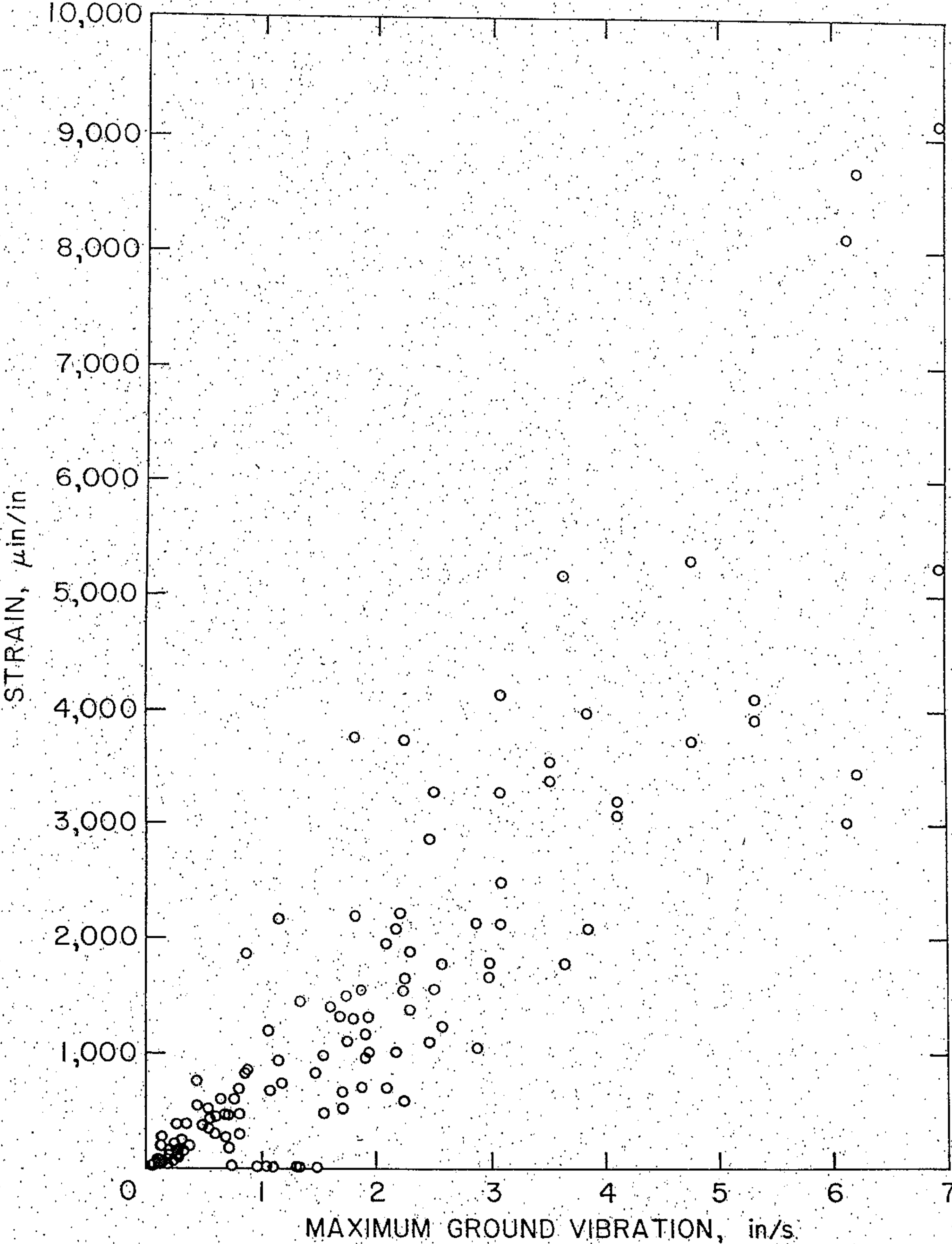

FIGURE 36. - Brick veneer joint strain versus maximum ground vibration.

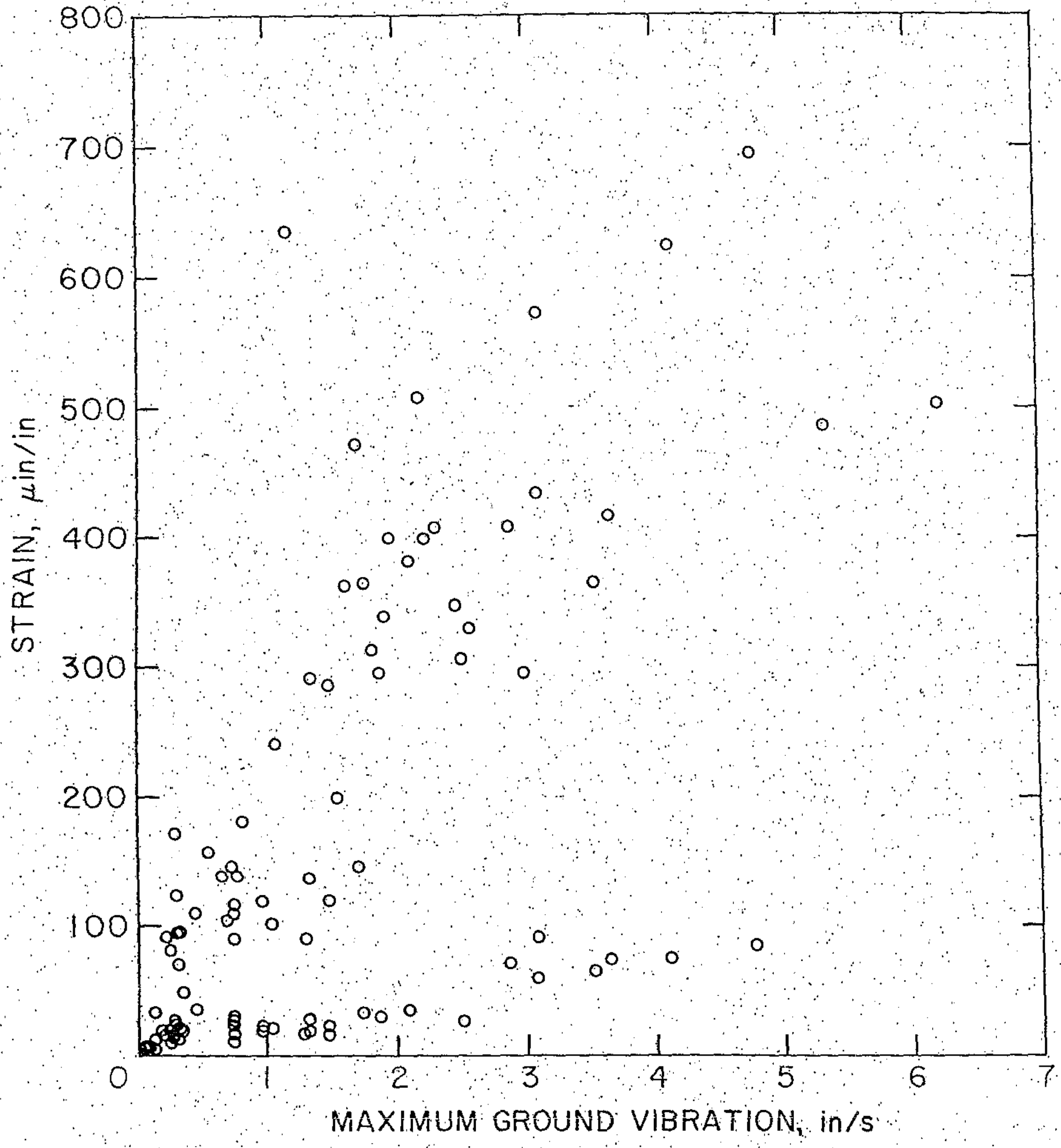

FIGURE 37. - Fireplace brick joint strain versus maximum ground vibration.

CRACKING OBSERVED IN TEST HOUSE

The methods used to observe cracking in the house depended on a number of factors. Regardless of the material, the first cracks became visible at widths of around 0.01 to 0.1 mm. The minimum widths at which cracks were detected varied, depending on the inspector and whether or not the trouble light was properly used. Cracks were difficult to find without proper sidelighting, and

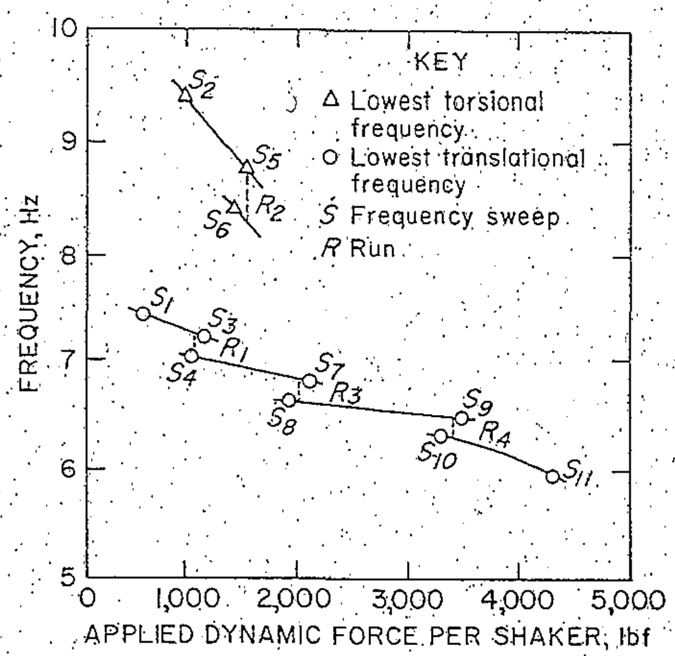

FIGURE 38. - Resonance frequencies versus applied dynamic force during shaker tests.

many that were found probably would not have been noticed by homeowners. With normal environmental cycling, these cracks widened over time and became clearly visible without sidelighting. Cracking at block joints was extremely difficult to quantify, since most areas already had shrinkage separation at the joints, as was found during the initial inspection. During blasting, one inspector examined specific areas in the concrete block basement for cracks, but various inspectors performed the semimonthly observations over the whole area. As a consequence, the concrete block cracking reports were disregarded for the semimonthly analysis.

Blast-Induced Cracking

Cracks observed from blasting are listed in table 11. These were determined from preblast and postblast inspections conducted within 1 h of shooting. Corner crack extensions appeared after shot 89, which produced a peak ground vibration of 0.88 in/s. With respect to cracking, wallboard corner joints were found to be the weakest areas in the test house. As previously mentioned, corner cracks are also caused by human activity in conjunction with material drying and shrinkage. At peak ground vibrations ranging from ~ 1.8 to 2.2 in/s, cracking of wallboard was limited to joint compound over nailheads.

Local cracks in masonry walls were observed at interfaces of mortar joints and bricks or concrete blocks at peak ground vibrations of ~ 3.4 and 6.2 in/s, respectively (table 11). A diagonal steplike crack in the southeast basement wall, starting at ground height and proceeding upwards, was observed after shot 48. At the time shots 45-48 were detonated, their vibration levels (ranging from ~ 1.0 to 1.5 in/s) were the highest recorded in the study. But because observation of cracks in masonry is difficult, it remains unknown whether blasting or other events caused this steplike crack.

Widening of wallboard and masonry cracks was observed to occur from both blasting and natural events. Often, barely visible cracks became clearly visible due to overnight environmentally induced stresses or upon inspection following a shot. It was not until shot 126 that blasting widened a crack beyond the width that would have occurred in the absence of a blast. The peak ground vibration for this shot was 6.94 in/s.

TABLE 11. - Cracks observed after blasting

Shot	Ground vibration level, in/s			Crack observation
	Vertical	East-west	North-south	
45...........	0.38	1.03	0.54	
46...........	.44	1.32	.71	
47...........	.48	1.47	.71	
48...........	.48	.96	.49	Diagonal steplike crack in concrete block wall. Found during detailed inspection after shot 48; unknown if existed prior to shots 45-58.
82...........	2.21	1.41	1.75	Crack in joint compound over nailhead.
83...........	3.05	2.75	1.64	Corner crack extension.
84...........	2.17	2.01	1.44	Crack in joint compound over nailhead.
86...........	.85	1.34	1.15	2 corner crack extensions.
89...........	.40	.88	.78	Corner crack extension.
97...........	1.17	1.11	1.81	Crack in joint compound over nailhead.
101...........	3.12	3.52	2.19	Corner crack extension.
102...........	4.77	3.21	4.25	Plywood subfloor crack.[1]
114...........	3.33	3.43	NA	Brick veneer mortar joint crack.
115...........	6.19	6.22	3.52	Basement block mortar joint cracks.
126...........	6.19	6.94	5.27	Chimney mortar cracks, all sides. Basement block mortar joint separation; minor damage.

NA Not available.
[1]Test house had subfloor only--no underlayment or finish floor.

Shaker-Induced Cracking

Cracking produced by mechanical cyclic loading is presented in table 12. As noted in the discussion of shaker-induced structure response, most wallboard cracking (other than at the corners) was limited to joint compound over nailheads. Additionally, one taped joint failed, and several brick and block mortar-joint crack extensions occurred. The total number of cycles for each occurrence of cracking, the last column of table 12, is based on the estimated total cycles induced by 2 yr of daily environmental changes (700), human activities (300), blasting at levels > ~ 0.5 in/s (500), and sweep tests (2,500/sweep at levels > ~ 0.5 in/s).

Since no strain gauges were installed at the site of the taped-joint crack, the dynamic shaker strain and prestrain levels are not known. However, data from the shaker tests (table 12) and the single fatigue test of wallboard discussed in appendix A (table A-6) confirm that many loading cycles are needed fatigue when wallboard is cyclically loaded at vibration levels equivalent to < 1 in/s ground vibration.

TABLE 12. - Cracks observed after shaker excitation

Shaker vibration equivalency[1] and crack description	Number of cycles at cracking	
	Run	Total[2]
Run 1, ~ 0.5 in/s:		
Entryway tape joint crack............	52,000	56,000
Crack in joint compound over nailhead in master bedroom..................	52,000	56,000
Fireplace mortar joint crack extension[3]........................	52,000	56,000
Run 2, ~ 0.5 in/s:		
Chimney trim broken loose from siding[3]...........................	>1	>108,500
Mortar joint crack at top of chimney.	>1	>108,500
Run 3, ~ 0.3 in/s:		
Brick veneer mortar joint cracks.....	15,000	229,500
4 cracks in joint compound over nailheads..........................	25,000	239,000
Run 4, ~ 0.75 in/s:		
Vertical crack through brick veneer mortar............................	14,500	293,500
Cracks in joint compound over nailheads..........................	60,000	339,500
Basement block mortar joint crack extensions.........................	>1	>339,500
Run 5, ~ 1.0 in/s:		
Brick veneer mortar falling out......	>1	>339,500
Basement block mortar joint crack extensions.........................	>1	>339,500
Crack in wallboard..................	22,000	361,500

[1]Based on envelope response from plot of ground vibration versus structure motion at site A_4 (fig. 13), high corner, east wall, as structure was at resonance.

[2]At vibration equivalency of ~ 0.5 in/s; including cycles induced by blasting and frequency sweeps.

[3]Cracking suspect because superstructure was racked against normally foundation-driven fireplace.

Shaker-induced masonry cracking occurred at brick or block mortar-joint interfaces. As mentioned, visible cracking is observed at displacements of 0.01 to 0.1 mm, which correspond to strains of 770 and 7,700 µin/in across joint widths of 13 mm. As is discussed in appendix A, overall wall integrity is heavily dependent on workmanship, and cracks of this width (0.01 to 0.1 mm) will inevitably be found after construction (32-34). Additional causes of cracks this size are mortar shrinkage, natural events, and/or vibrations. No steplike crack propagations were observed across brick or block walls. The existing steplike crack in the southeast basement wall (discussed in "Blast-Induced Cracking" section) functioned as an area of strain relief during shaker runs. Energy transmitted by the shakers into the superstructure and foundation was dissipated in areas of previous cracking. Therefore, new cracks observed during the shaker tests were primarily extensions of cracks that had already occurred.

Long Term Cracking Observations

Cracks observed in the test house during the semimonthly inspections are listed in table 13. The crack rate, or number of new cracks per inspection, along with the number of blasts that produced

TABLE 13. - Cracks observed during semimonthly inspections

Inspection period	Date	Brick veneer joints	Fireplace chimney joints	Wallboard	Wallboard joints	Corners	Nail pops
Initial..........	10/18/79	20	21	3	2	6	5
1..............	10/30/79	ND	8	ND	ND	ND	ND
2..............	11/13/79	ND	ND	ND	ND	6	ND
3..............	11/27/79	ND	ND	ND	ND	ND	ND
4..............	12/13/79	ND	ND	ND	ND	ND	ND
5..............	12/28/79	ND	ND	1	ND	ND	ND
6..............	1/ 9/80	3	ND	ND	ND	4	ND
7..............	1/24/80	ND	ND	ND	ND	ND	ND
8..............	2/12/80	ND	ND	ND	ND	ND	ND
9..............	2/26/80	ND	ND	ND	ND	ND	ND
10..............	3/13/80	ND	ND	1	3	ND	ND
11..............	3/27/80	ND	1	ND	ND	3	ND
12..............	4/10/80	ND	ND	ND	ND	1	ND
13..............	4/25/80	ND	ND	ND	ND	ND	ND
14..............	5/ 7/80	ND	ND	ND	ND	2	ND
15..............	5/22/80	6	ND	ND	1	38	ND
16..............	6/ 6/80	ND	ND	ND	ND	1	ND
17..............	6/25/80	ND	ND	ND	ND	1	ND
18..............	7/15/80	ND	ND	ND	ND	0	ND
19..............	7/30/80	ND	ND	ND	ND	1	ND
20..............	8/19/80	ND	ND	ND	1	2	ND
21..............	8/28/80	ND	ND	ND	ND	1	ND
22..............	9/15/80	ND	ND	ND	ND	5	ND
23..............	9/30/80	ND	ND	ND	ND	ND	ND
24..............	10/10/80	ND	ND	ND	ND	1	ND
25..............	10/24/80	ND	ND	ND	ND	ND	ND
26..............	11/11/80	ND	ND	ND	ND	ND	ND
27..............	11/21/80	ND	ND	1	ND	5	ND
27[1]..............	12/ 1/80	ND	ND	ND	ND	2	ND
28..............	12/ 9/80	ND	ND	ND	ND	5	ND
29..............	12/17/80	ND	ND	ND	ND	2	ND
30..............	1/13/81	ND	ND	1	ND	1	ND
31..............	1/27/81	ND	ND	2	1	ND	ND
32..............	2/13/81	6	ND	ND	ND	ND	ND
33..............	3/ 3/81	ND	ND	ND	ND	ND	ND
34..............	3/18/81	ND	ND	ND	ND	ND	1
35..............	4/14/81	ND	ND	ND	ND	ND	ND
36..............	4/28/81	5	1	ND	ND	ND	ND
37..............	5/28/81	ND	ND	ND	ND	ND	ND
38..............	6/18/81	ND	ND	ND	ND	ND	ND
39..............	7/ 1/81	ND	ND	ND	ND	ND	ND
40..............	7/16/81	ND	ND	ND	ND	ND	ND
41..............	7/30/81	ND	ND	ND	ND	ND	ND
42[1]..............	8/14/81	ND	ND	ND	ND	1	ND
42..............	8/18/81	ND	ND	ND	ND	1	ND
43..............	8/28/81	ND	ND	ND	ND	ND	ND
44..............	9/17/81	ND	ND	ND	ND	ND	ND
44[1]..............	9/23-25/81	8	ND	ND	ND	3	1
45..............	10/ 1/81	ND	ND	ND	ND	1	ND
46..............	10/15/81	ND	ND	ND	ND	ND	ND
47..............	11/ 3/81	ND	ND	ND	ND	2	5

ND None detected. [1]Dynamic blast inspection.

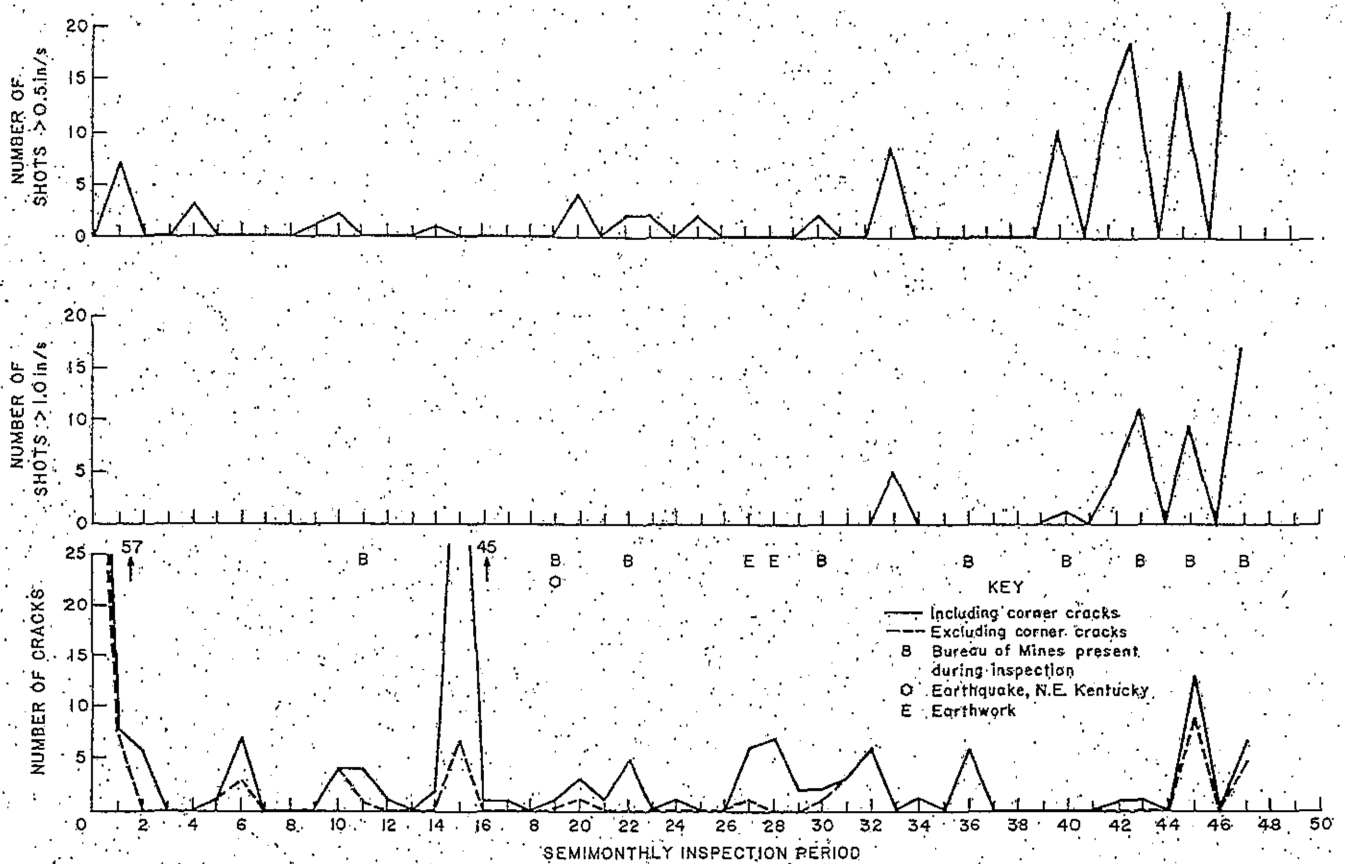

FIGURE 39. - Number of cracks and blasts >0.50 in/s and >1.0 in/s versus inspection period.

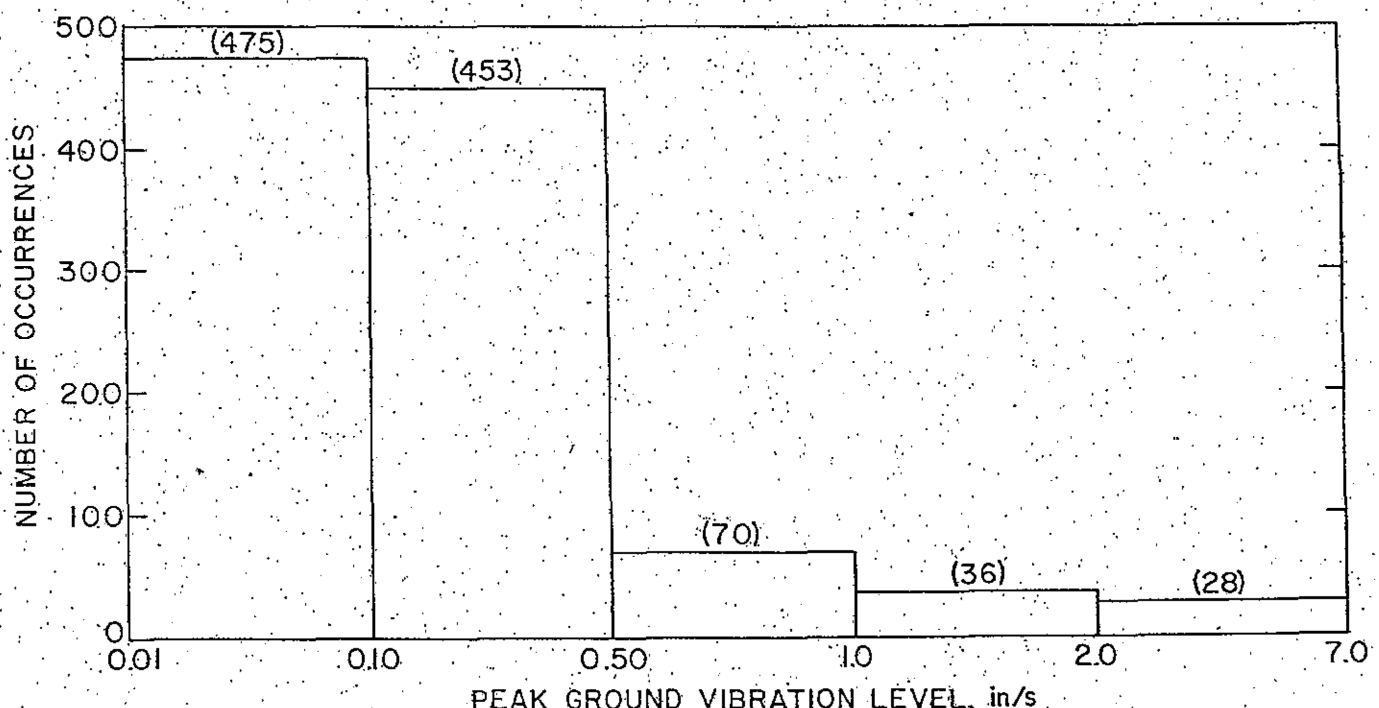

FIGURE 40. - Histogram of peak ground vibration levels recorded at test house.

ground vibrations >0.50 in/s and >1.0 in/s, is shown in figure 39. The histogram of all peak ground vibration levels is shown in figure 40. The ground vibration levels were either recorded by the self-triggering equipment or back calculated using propagation equations in the 0.01- to 0.10-in/s range. (Of the 475 vibration levels in this range, 250 were calculated.)

Some of the crack rates shown in figure 39 include small hairline corner cracks, and some do not. The majority of corner cracks occurred in the first 8 months. Cracks were found in nearly every corner in the house, but were ignored up to inspection period 15. Then it was decided to rigorously observe them despite their miniscule size. Corner cracks are an inevitable consequence of the curing of the tape compound and are enhanced by dynamic strains induced by human activity.

Differences were found in the number of cracks observed by the two teams of inspectors (VME and Bureau personnel) during periods 1, 15, and 36. The most pronounced difference was for period 15. The decision to include small corner cracks was made after VME had completed its inspection for that period but before the Bureau had completed its inspection for period 15. Otherwise, differences in the number of cracks observed were an inevitable consequence of the difficulty of observing hairline-width (0.01 to 0.1 mm) cracks. Periods 1, 15, and 36 were omitted in calculations of crack rates. Periods with unusual external influences, including an earthquake and soil removal by a scraper 40 ft from the test house, were included. The self-triggering seismograph recorded a 0.06-in/s vibration for the scraper activity but did not trigger during the earthquake. Strain measurements did not vary from normal fluctuations during the earthquake.

Crack rates during periods of high- and low-level ground vibration are compared in table 14. Two methods were used for interpreting this data. In the first, it was assumed that blasting is fatigue-damaging in nature (i.e., it lowers strain levels necessary for failure). In the second method, it was assumed that blasting produces a triggering strain (which when added to an existing strain exceeds the critical strain). The first method required investigation of consecutive inspection periods, since high crack rates may occur even during nonblast periods. For both methods, a ground vibration level of 0.5 in/s was chosen as the lowest vibration level for study because a 0.59-in/s vibration was found to produce the same strain level as normal household activities (table 9). A velocity of 1.0 in/s was chosen for the upper bound because there were insufficient data at higher levels.

The number of new cracks per week did not increase with time, indicating that blast vibrations do not cause fatigue-related damage. Results interpreted using the second method indicated that ground vibrations >1.0 in/s were associated with crack rates of 1.8 cracks per week, while vibrations <1.0 in/s were associated with rates of 0.9 cracks per week. The increase in crack rate with ground vibration level indicates that blasting does produce a triggering strain, at about 1.0 in/s.

The low crack-formation rates reported are reasonable since the test house was new, showed no differential settlement, and was not regularly occupied. These conditions result in low natural crack-formation rates, which allow the greatest sensitivity to the appearance of only a few blast-related cracks. In other words, the low natural crack rates found in these tests allowed a few blast-related cracks to significantly affect crack-formation rates.

TABLE 14. - Crack rate versus blast vibration level

Blast vibration level, in/s	Inspection periods[1]	Number of cracks per week[2]	
		Total	Excluding corner cracks
METHOD 1 (FATIGUE DAMAGING; ACCUMULATIVE WEAKENING OF MATERIAL)			
>1.0	40-47	1.4	0.88
<1.0	1-14	1.2 (0.96)	.61 (0.35)
	16-32	1.1	.35
>0.5, <1.0	1-14	1.2 (.96)	.61 (.35)
	20-32	1.4	.46
METHOD 2 (TRIGGERING EFFECT; SUM OF DYNAMIC AND EXISTING STRAIN IN EXCESS OF THRESHOLD)			
>1.0	33, 40, 42-43, 45, 47	1.8	1.0
<1.0	1-14, 16-32, 34-35, 37-39, 41, 44, 46	.94 (0.86)	.38 (0.29)
>0.5, <1.0	1, 4, 9-10, 14, 20, 22-23, 25, 30	1.2 (.89)	.70 (.33)
<.50	2-3, 5-8, 11-13, 16-19, 21, 24, 26-29, 31-32, 34-35, 37-39, 41, 44, 46	.84	.28

[1]Periods listed in table 13; 2 weeks each.
[2]Values in parentheses are rates calculated without period-1 data to account for cracks resulting from curing after construction.

SUMMARY AND CONCLUSIONS

A full-scale residential test house was subjected to 2 yr of vibration produced by adjacent surface mining. For the first time, the strain response of a house was fully documented. Long term strain measurements allowed the blast-induced strains to be compared with those produced by changes in environmental factors such as temperature, humidity, and human activity. Continued visual inspections for cracks during the 2-yr period allowed the calculation of crack-formation rates for correlation with vibration levels. After the study of blast-induced cracks was completed, the entire house was shaken mechanically to determine the threshold of fatigue cracking of the wall coverings. Laboratory tests were conducted to aid in evaluation of the field observations. The following conclusions are based upon the observations made during this full-scale field study:

Crack Appearance

Numerous hairline cracks, ~ 0.01 to 0.1 mm wide, appeared in the test house during construction. Cracks of this size are difficult to see and are usually not noticed by the homeowner. Wallboard cracks from blasting occurred primarily in corners and around nailheads in the joint compound. One hairline crack in a wall corner extended after a blast that produced a peak ground vibration of 0.88 in/s. This was the lowest observed vibration that modified an existing crack pattern. Wallboard cracks also appeared, widened, and/or extended during periods of no blasting. Thus, other phenomena also caused, widened, and extended these cracks. Therefore, observations of cracking are better evaluated in terms of the number of new cracks observed per time interval rather than the number of cracks seen at a single inspection.

Blast-induced local masonry cracking along mortar joint and block interfaces was hard to distinguish from the numerous preexisting cracks that resulted from shrinkage and workmanship. A diagonal steplike crack across the southeast basement wall, which was found after four shots ranging from 1.0 to 1.5 in/s, was more readily observed.

Strains Associated With Cracking

Laboratory tests and previous studies indicate that the initial paper failure of gypsum wallboard occurs at a strain of approximately 1,000 µin/in and that visible cracks appear at strains slightly beyond this point. Concrete block shows visible localized cracks at mortar-joints strains of approximately 3,000 µin/in when a gauge width of 13 mm is used. Global strain appears to be the best predictor of diagonal steplike cracks. Confirmation of these results and further definition of threshold levels are anticipated from wall testing planned by the National Bureau of Standard (NBS) for fiscal 1984.

Wall Strains Associated With Environmental Factors

Temperature- and humidity-induced strains across wallboard taped joints were as high as 149 and 385 µin/in. Door slamming produced strains of up to 140 µin/in in wallboard.

Wall Strains Associated With Blasting

The smallest ground vibrations that would produce the equivalent of environmental and door-slamming strains in walls are 1.2 and 0.5 in/s, respectively.

Fatigue Tests--Wall Board

Mechanical vibration cracked a wallboard tape joint after 52,000 cycles of motion at strain levels in the house equivalent to those resulting from a blast with a peak ground vibration of ~ 0.5 in/s. Adding 4,000 cycles for environmentally induced strains brings the number of cycles at failure to 56,000. Assuming 200 workdays per year × 2 shots per day × 5 cycles per shot, this shaking was equivalent to subjecting the house to 28 yr of blasting twice a day.

Fatigue Tests--Masonry Walls

Because of the cracked condition of the masonry walls at the test house, cyclic tests were conducted with NBS using other test walls. Fatigue effects appeared minor until stress levels were near ultimate capacity, but further analysis awaits the 1984 tests mentioned earlier.

Crack Rate

Threshold-type cracks appeared with and without blasting. Therefore, changes in the rate of threshold crack occurrences are better indicators of the effects of blasting on cracking than observations of individual cracks. The rate of threshold cracking when ground motions were <0.5 in/s was not significantly different than when motions were between 0.5 and 1.0 in/s. However, when ground motions exceeded 1.0 in/s, the rate of crack formation was more than three times the rate observed when motions were <1.0 in/s.

REFERENCES

1. Siskind, D. E., V. J. Stachura, M. S. Stagg, and J. W. Kopp. Structure Response and Damage Produced by Airblast From Surface Mining. BuMines RI 8485, 1980, 111 pp.

2. Siskind, D. E., M. S. Stagg, J. W. Kopp, and C. H. Dowding. Structure Response and Damage Produced by Ground Vibration From Surface Mining Blasting. BuMines RI 8507, 1980, 74 pp.

3. Andrews, D. K., G. W. Zumwalt, R. L. Lowery, J. W. Gillespie, and D. R. Low. Structure Response to Sonic Booms. (U.S. FAA contract FA-64-AC-6-526, Andrews Associates Inc. and Hudgins, Thompson, Ball and Associates Inc., Oklahoma City, OK). Rep. AD610822, Feb. 5, 1965, 228 pp.; available from Defense Documentation Cent., Cameron Sta., Bldg. 5, 5010 Duice St., Alexandria, VA 22314.

4. Crockett, J. H. Presentation of Structural Failures by Repeated Vibration Loading. Paper in Proc. Int. Conf. on Performance of Building Structures, Glasgow Univ., Mar. 31-Apr. 1, 1976. Pentech Press, 1976, pp. 201-228.

5. Dowding, C. H., W. K. Beck, and D. K. Atmatzidis. Blast Vibration Implications of Cyclic Shear Behavior of Model Plaster Panels. Geotech. Testing J., ASTM, v. 3, No. 2, June 1980, pp. 80-88.

6. Leigh, B. R. Lifetime Concept of Plaster Panels Subjected to Sonic Boom. University of Toronto, Canada, UTIAS-TN-191, July 1947, 78 pp.

7. Hidalgo, P. A., R. L. Mayes, H. D. McGiven, R. W. Clough. Cyclic Loading Tests of Masonry Single Piers. Height to Width Ratio of 0.5, v. 3. Coll. Eng., Univ. CA, Richmond, CA, Rep. UCB/EERC-79/12 (to Natl. Sci. Found., May 1979, 144 pp.; NTIS PB 301 321.

8. Koerner, R. M., and J. L. Rosenfarb. Feasibility of Fatigue Assessment of Block Walls From Laboratory Scale Methods. (contract J0285013). BuMines OFR 144-80, 1980, 96 pp.; NTIS PB 81-140139.

9. Mayes, R. L., Y. Omote, and R. W. Clough. Cyclic Shear Tests of Masonry Piers. Test Results, v. 1. Coll. Eng., Univ. CA, Berkeley, CA, Rep. EERC 76-8 (to Natl. Sci. Found.), May 1976, 84 pp.; Springfield, VA, NTIS PB 264 424.

10. McNatt, J. Dobbin. Design Stresses for Hardboard-Effect of Rate, Duration, and Repeated Loading. For. Prod. J., v. 20, No. 1, pp. 53-59.

11. Woodward, K. A., and F. Rankin. Behavior of Concrete Block Masonry Walls Subjected to Repeated Cyclic Displacements. NBSIR 83-2780, 1983, 178 pp.; NTIS PB 84-122092.

12. Sabnis, G. M. Vibrations of Concrete Structures. Introduction and Background. Am. Concrete Inst., SP-60, 1979, pp. 1-12.

13. Tuomi, R. L., and W. J. McCutcheon. Testing of a Full-Scale House Under Simulated Snowloads and Windloads. USDA Forest Service Res. Paper FPL 234, 1974, 32 pp.

14. Warwaruk, J. Vibrations of Concrete Structures. Defection Requirements--History and Background Related to Vibrations. Am. Concrete Inst., SP-60, 1979, pp. 13-41.

15. Whittemore, H. L., J. B. Cotter, A. H. Stang, and V. B. Phelan. Strength of Houses--Application of Engineering Principles to Structural Design. NBS Bldg. Mater. and Structures Rep. BMS 109, Apr. 1948, 131 pp.; NTIS Com-73-10986.

16. Crist, R. A., and J. A. Shaver. Vibrations of Concrete Structures. Development of Model Performance Criteria for Deflection of Concrete Floors. Am. Concrete Inst., SP-60-3, 1979, pp. 43-66.

17. International Standards Organization. Guide for the Evaluation of Human Exposure to Whole-Body Vibration. ISO 2631-1978 (E), 1978, 15 pp.

18. American National Standards Institute. Guide to the Evaluation of Human Exposure to Vibration in Buildings. ANSI S3.29-1983 (Acoust. Soc. Am., ASA 48-1983), 1983, 10 pp.

19. Beck, W. K. Fatigue Cracking of Drywall To Model Blast Loading. M.S. Thesis, Northwestern Univ., Evanston, IL, June 1979, 131 pp.

20. Building Research Establishment. Cracking in Buildings. Dig. 75, Oct. 1975, pp. 1-7.

21. Thoenen, J. R., and S. L. Windes. Seismic Effects of Quarry Blasting. BuMines 442, 1942, 83 pp.

22. Wiggins, J. H., Jr. Effects of Sonic Boom. J. H. Wiggins, July 1969, 174 pp.

23. Brun, R. W., R. C. Speck, W. C. McCann, and O. S. Cecil. Survey of Ground Surface Conditions Affecting Structural Response to Subsidence. (contract J0295014, GAI Consultants, Inc.). BuMines OFR 12-84, 1983, 602 pp.; NTIS PB 84-1555860.

24. Byrd, V. Effect of Relative Humidity Changes During Creep on Handsheet Paper Properties. Tappi, v. 55, No. 2, pp. 247-252.

25. ____. Effect of Relative Humidity Changes on Compressive Creep Response of Paper. Tappi, v. 55, No. 11, pp. 1612-1613.

26. Wink, W. A. The Effect of Relative Humidity and Temperature on Paper Properties. Tappi, v. 44, No. 6, pp. 171A-178A.

27. Holmberg, R., N. Lundberg, and G. Rundqvist. Ground Vibration and Damage Criteria. Construction Res. Council, Stockholm, Sweden, Rep. R 85:81, 1981, 30 pp.

28. Wall, J. R., Jr. Seismic-Induced Architectural Damage to Masonry Structures at Mercury, Nevada. Bull. Seismol. Soc. Am., v. 57, No. 5, pp. 991-1007.

29. Stagg, M. S., and A. J. Engler. Ground Vibration Measurement and Seismograph Calibration. BuMines RI 8506, 1980, 62 pp.

30. Stachura, V. J., D. E. Siskind, and A. J. Engler. Airblast Instrumentation and Measurement Techniques for Surface Mine Blasting. BuMines RI 8508, 1981, 53 pp.

31. Crawford, R., and H. S. Ward. Dynamic Strains in Concrete and Masonry Walls. Can. Natl. Res. Council, Div. Bldg. Res., Ottawa, Ontario, Bldg. Res. Note 54, Dec. 1965, 13 pp.

32. Cranston, W. B. Masonry Research and Codes in the United Kingdom. Paper in Earthquake Resistant Masonry Construction: National Workshop (NBS, Boulder, CO, Sept. 13-16, 1976), ed. by R. A. Crist and L. E. Cattaneo, NBS Bldg. Sci. Series 106, Sept. 1977, pp. 166-176.

33. Green, D. G., I. A. Macleod, and W. G. Stark. Observation and Analysis of Brick Structures on Soft Clay. Paper in Proc. Int. Conf. on Performance of Building Structures, Glasgow Univ., Mar. 31-Apr. 1, 1976. Pentech Press, 1976, pp. 321-336.

34. Wroth, C. P. General Report Session IIIA: Response of the Structure to Foundation Movements. Paper in Proc. Int. Conf. on Performance of Building Structures, Glasgow Univ., Mar. 31-Apr. 1, 1976. Pentech Press, 1976, pp. 489-508.

35. Wiss, J. F., and H. R. Nicholls. A Study of Damage to a Residential Structure From Blast Vibrations. Res. Council for Performance of Structures, ASCE, New York, 1974, 73 pp.

36. Scott, J. L. (U.S. Gypsum Co.). Physical Properties--1/2" Gypsum Panels. Private communication, 1982; available upon request from M. S. Stagg, BuMines, Minneapolis, MN.

37. Brezinski, J. P. The Creep Properties of Paper. Tappi, v. 39, No. 2, pp. 116-128.

38. Coleman, B. D. Time Dependance of Mechanical Breakdown Phenomena. J. Appl. Phys., v. 27, No. 8, pp. 862-866.

39. Coleman, E. I. Application of the Theory of Absolute Reaction Rates to the Creep Failure of Polymeric Filaments. J. Polym. Sci., v. 20, 1956, pp. 447-455.

40. Fulmer, G. E., and J. L. Guthrie. Flex Life and Long Term Strength of Composite Materials. J. Appl. Polym. Sci., v. 13, 1969, pp. 445-458.

41. Guthrie, G. E., and G. E. Fulmer. Characterization of Saturated Cellulosic Webs by the Creep Failure Method. Tappi, v. 52, No. 11, pp. 2181-2190.

42. Kallmes, O., G. Bernier, M. Perez. A Mechanistic Theory of the Load-Elongation Properties of Paper (in four parts). Pap. Technol. and Ind., v. 18, Nos. 7-10, 1977, pp. 222-228, 243-246, 283-285, 328-331.

43. Prevorsek, D., and W. James Lyons. Fatigue Fracture in Fibrous Polymers as a Brittle, Crack-Nucleation Process. J. Appl. Phys., v. 35, No. 11, pp. 3152-3164.

44. Seth, R. S. Measurement of Fracture Resistance of Paper. Tappi, v. 62, No. 7, pp. 92-95.

45. Wink, W. A., K. W. Hardacker, R. H. Van Eperen, and J. A. Van Den Akker. The Effect of Initial Span on the Measured Tensile Properties of Paper. Tappi, v. 47, No. 1, pp. 47-54.

46. Fattal, S. G. The Capacity of Unreinforced Masonry Walls Under Membrane Loads. Paper in Earthquake Resistant Masonry Construction: National Workshop (NBS, Boulder, CO, Sept. 13-16, 1976), ed. by R. A. Crist and L. E. Cattaneo, NBS Sci. Series 106, Sept. 1977, pp. 177-197.

47. Fattal, S. G., and L. E. Cattaneo. Structural Performance of Masonry Walls Under Compression and Flexure. NBS Bldg. Sci. Series 73, June 1976, 65 pp.

48. Hegemier, G. A., G. Kushnamoorthy, and R. O. Nunn. An Experimental Study of Concrete Masonry Under Seismic-Type Loading. Paper in Earthquake Resistant Masonry Construction: National Workshop (NBS, Boulder, CO, Sept. 13-16, 1976), ed. by R. A. Crist and L. E. Cattaneo, NBS Sci. Series 106, Sept. 1977, pp. 114-153.

49. Mayes, R. L., and R. W. Clough. State-of-the-Art in Seismic Shear Strength of Masonry—An Evaluation and Review. Coll. Eng., Univ. CA, Berkeley, CA, Rep. EERC 75-21 (to Nat. Sci. Found., Oct. 1975, 137 pp.; NTIS PB 249 040.

50. Mayes, R. L., R. W. Clough, and Y. Omote. Seismic Research on Masonry. Paper in Earthquake Resistant Masonry Construction: National Workshop (NBS, Boulder, CO, Sept. 13-16, 1976), ed. by R. A. Crist and L. E. Cattaneo, NBS Sci. Series 106, Sept. 1977, pp. 61-90.

51. Mayes, R. L., R. W. Clough, Y. Omote, and S. W. Chen. Expected Performance of Uniform Building Code Designed Masonry Buildings. Paper in Earthquake Resistant Masonry Construction: National Workshop (NBS, Boulder, CO, Sept. 13-16, 1976), ed. by R. A. Crist and L. E. Cattaneo, NBS Sci. Series 106, Sept. 1977, pp. 91-113.

52. Omote, Y., R. L. Mayes, S. W. Chen, and R. W. Clough. A Literature Survey—Transverse Strength of Masonry Walls. Coll. Eng., Univ. CA, Berkeley, CA, Rep. UCB/EERC-77/07 (to U.S. Dep. Hous. and Urban Dev.), Mar. 1977, 137 pp.; NTIS PB 277 933.

53. Whittemore, H. L., A. H. Stang, and D. E. Parsons. Structural Properties of Six Masonry Wall Constructions. NBS Bldg. Mater. and Structures Rep. BMS 5, Nov. 1938, 31 pp.; NTIS Com-73-10943.

54. ______. Structure Properties of Two Brick-Concrete-Block Wall Constructions and a Concrete-Block Wall Construction. (Sponsored by Natl. Concr. Masonry Assoc.). NBS Bldg. Mater. and Structures Rep. BMS 32, Nov. 2, 1939, 21 pp.; NTIS COM-73-10948.

55. Yokal, F. Y., R. G. Mathey, and R. D. Dikkers. Strength of Masonry Walls Under Compressive and Transverse Loads. NBS Bldg. Sci. Series 34, Mar. 1971, 74 pp.

56. Mayes, R. L., and R. W. Clough. A Literature Survey—Compressive, Tensile, Bond and Shear Strength of Masonry. Coll. Eng., Univ. CA, Berkeley, CA, Rep. EERC 75-15 (to Nat. Sci. Found.), June 1975, 199 pp.; NTIS Service, Springfield, VA, PB 246 292.

57. Haldane, D. The Importance of Cracking in Reinforced Concrete Members. Paper in Proc. Int. Conf. on Performance of Building Structures, Glasgow Univ., Mar. 31-Apr. 1, 1976. Pentech Press, 1976, pp. 99-109.

58. Edwards, A. T., and T. D. Northwood. Experimental Studies of the Effects of Blasting on Structures. Engineer, v. 210, Sept. 30, 1960, pp. 538-546.

59. Northwood, T. D., R. Crawford, and A. T. Edwards. Blasting Vibrations and Building Damage. Engineer, v. 215, No. 5601, May 31, 1963, pp. 973-978.

60. Atkins, K. P., Jr., and D. E. Dixon. Vibrations of Concrete Structures. Concrete Structures and Construction Vibrations. Am. Concrete Inst., SP-60-10, 1979, pp. 213-247.

61. Woodward, K. (NBS). Private communication, 1983; available on request from M. S. Stagg, BuMines, Minneapolis, MN.

62. Nelson, W. H. Movement of Building Element Cracks in Six Mercury Nevada Structures. (U.S. AEC contract At-(26-1)-99, John A. Blume and Associates, Res. Div.). Rep. NVO-99-20, Dec. 1957, 45 pp.

63. Lenczner, D. Creep and Moisture Movements in Brickwork and Blockwork. Paper in Proc. Int. Conf. on Performance of Building Structures, Glasgow Univ., Mar. 31-Apr. 1, 1976. Pentech Press, 1976, pp. 369-383.

64. Thomas, K. The Performance of High Rise Masonry Structures. Paper in Proc. Int. Conf. on Performance of Building Structures, Glasgow Univ., Mar. 31-Apr. 1, 1976. Pentech Press, 1976, pp. 87-98.

APPENDIX A.--FAILURE OF WALLBOARD AND MASONRY WALLS

Analysis of wallbord failure data for a previous study (2) produced several questions. An expanded wallboard testing program was developed to identify core failure and examine the large variation of strain readings, the effect of strain rate and measurement method on strain readings, cyclic response, and the relative strength contributions of the composite materials. Additionally, cyclic and monotonic shear tests were conducted with the National Bureau of Standards (NBS) on 5- by 5-ft masonry walls and corner walls with 3-1/2-ft legs (11). Each material is discussed below with regard to elastic response to failure and nonlinear response during the time when cracks were widening to the point at which visual observation became possible.

Wallboard

Modern houses typically have interior walls of gypsum wallboard, also called gypsum board, Sheetrock, and Drywall. Wallboard is a composite material consisting of a core of gypsum plaster of variable thickness bonded on both sides by smooth 0.015-in-thick paper. Although not considered a structural material, wallboard is often stressed and sometimes visibly cracked. Table A-1 lists bending, shear, and tensile strains of wallboard and related materials at failure as reported in previous studies (2, 6, 10, 35-36). Core failure for both bending (34) and tensile stresses (2) was identified at ~ 1,000 µin/in in RI 8507 (2). Tensile failure tests on gypsum core conducted by Beck (19) showed failure to occur at ~ 350 µin/in. Because of these differences, additional data were sought by running further tests on both wallboard and wallboard paper.

Paper tests were conducted following American Society for Testing and Materials (ASTM) standard test method D 828-60, "Tensile Breaking Strength of Paper and Paperboard," using an Instron model TM 100-kg, universal testing machine (fig. A-1). Wallboard and wallboard paper samples were kept in the same environment for 2 months prior to testing. This allowed a relative evaluation of failure properties.

Wallboard tensile tests were conducted on a 250-lbf MTS Systems Corp. electrohydraulic Servocontrol loading frame (fig. A-2). Load rates varied from 0.00008 to 0.2 in/s. Conversion of failure time to frequency, assuming 1/4 wavelength at failure, gave frequencies of 5 to 0.002 Hz. Strain detectors were mounted across the center of the specimen (fig. A-3), and output was recorded and processed on the system described in RI 8507. Tests were run on notched and unnotched samples. Notched samples were used to determine effects of gauge length and positioning; the specimens were notched to induce failure at the strain-sensing location. Unnotched samples gave the data used to determine absolute failure levels. Specimen size was based on end constraints that exist in a house (i.e., panel size over a doorway or window of approximately 12 by 16 in) and the loading frame's size limitations. Strain gauges were glued to the sample with adhesive, and mounting bases for the strain-leaf and Kaman displacement systems were attached with a fast-drying epoxy. The cyclic response of the loading frame system and test apparatus was limited to 2 Hz, and the maximum strain produced was ~ 50 µin/in.

Cyclic strain readings from the measurement systems with varying gauge lengths are listed in table A-2. Although the various methods and lengths gave consistent results, an increase in load induced core failure and resulted in strain localization in the paper covering. The post-mounted strain systems produced reasonable results, but some error resulted because of the relatively large size of the mounting base. A smaller diameter mounting base would increase the accuracy but would be difficult to install. Figure A-4 shows the details of the post-mounted system.

TABLE A-1. - Failure characteristics of plaster, wallboard, and hardboard[1]

Investigator and type of failure	Material	Thickness, in	Prestrain, pct	Strain, µin/in	Stress	Cycles to failure	Time to failure
Leigh (6), tensile	Plaster beam	NA	0	460	300 lbf/in^2	1/4 (static).	NA.
	...do	3/8	0	365	300 lbf/in^2	1	NA.
	...do	3/8	0	260	200 lbf/in^2	10,000	33.3 min.
Wiss (35), bending	Gypsum wallboard, longitudinal section	3/8	0	[2]1,230	[2]920 lbf/in^2	1/4 (static).	
	...do	3/8	0	[3]3,300	[3]1,450 lbf/in^2	...do	NA.
	...do	1/2	0	[2]1,100	[2]650 lbf/in^2	...do	NA.
	...do	1/2	0	[3]4,700	[3]1,100 lbf/in^2	...do	NA.
	Gypsum wallboard, transverse section	3/8	0	[2]840	[2]580 lbf/in^2	...do	NA.
	...do	3/8	0	[3]3,770	[3]785 lbf/in^2	...do	NA.
	...do	1/2	0	[2]910	[2]380 lbf/in^2	...do	NA.
	...do	1/2	0	[3]2,400	[3]580 lbf/in^2	...do	NA.
	Gypsum wallboard	NA	NA	1,160	NA	NA (blasting)	NA.
Beck (19), shear	Gypsum wallboard core with paper laminate removed	5/8	0	[4]130	NA	1/4 (static).	NA.
	...do	5/8	0	80 (62 pct)	NA	[5]1,000	1.67 min.
	...do	5/8	0	50 (38 pct)	NA	[5]18,000	30 min.
	...do	5/8	20 (26 µin/in)	90 (69 pct)	NA	[5]330	33 s.
	...do	5/8	20 (26 µin/in)	76 (58 pct)	NA	[5]1,900	3.17 min.
	...do	5/8	20 (26 µin/in)	56 (43 pct)	NA	[5]8,500	14.2 min.
	Gypsum wallboard	5/8	20 (26 µin/in)	[2]340	NA	1/4 (static).	NA.
	...do	5/8		[3]>1,400	NA	...do	NA.
Bureau of Mines (2), tensile	...do	3/8	0	[6]1,240	[6]285 lbf/in^2	...do	NA.
	...do	3/8	0	[3]3,400	[3]285 lbf/in^2	...do	NA.
	...do	1/2	0	[6]1,420	[6]170 lbf/in^2	...do	NA.
	...do	1/2	0	[3]3,210	[3]250 lbf/in^2	...do	NA.
	...do	5/8	0	[6]1,445	[6]140 lbf/in^2	...do	NA.
	...do	5/8	0	[3]3,450	[3]230 lbf/in^2	...do	NA.
U.S. Gypsum Co. (36):							
Tensile	Gypsum wallboard, transverse section	1/2	0	NA	80 lb/in width	...do	NA.
	Gypsum wallboard, longitudinal section	1/2	0	NA	180 lb/in width	...do	NA.
Shear	Gypsum wallboard	1/2	0	NA	50 lbf/in^2	...do	NA.
Compressive	...do	1/2	0	NA	600 lbf/in^2	...do	NA.
McNatt (10), tension	Tempered hardboard	1/4	0	NA	90 pct[7]	...do	4.17 min.
	...do	1/4	0	NA	85 pct[7]	...do	15 min.
	...do	1/4	0	NA	80 pct[7]	...do	75 min.
	...do	1/4	0	NA	70 pct[7]	...do	23.6 h.
	...do	1/4	0	NA	60 pct[7]	...do	12.7 days.
	...do	1/4	0	NA	55 pct[7]	...do	81.0 days.
	...do	1/4	0	NA	50 pct[7]	...do	347 days.
	...do	1/4	49.5	NA	85 pct[7]	[8]100	6.6 s.
	...do	1/4	46.8	NA	80 pct[7]	[8]450	30 s.
	...do	1/4	44	NA	80 pct[7]	[8]1,200	1.33 min.
	...do	1/4	38.5	NA	70 pct[7]	[8]7,000	7.83 min.
	...do	1/4	33	NA	60 pct[7]	[8]75,000	1.39 h.
	...do	1/4	30.3	NA	55 pct[7]	[8]300,000	5.56 h.
	...do	1/4	27.5	NA	50 pct[7]	[8]1,100,000	20.3 h.

NA Not available.
[1]From laboratory tests, except that last line of data from Wiss was from in situ test.
[2]Core failure.
[3]Ultimate failure; paper laminate damage.
[4]Measured on test sample; other investigators used platen displacement.
[5]Cycled at 10 Hz.
[6]Reported in RI 8507 as core failure, but new analysis indicates initial paper failure.
[7]Percent of stress at failure, defined as the ratio of load at failure to load at failure at uniform rate of 1 in/min.
[8]Cycled at 15 Hz.

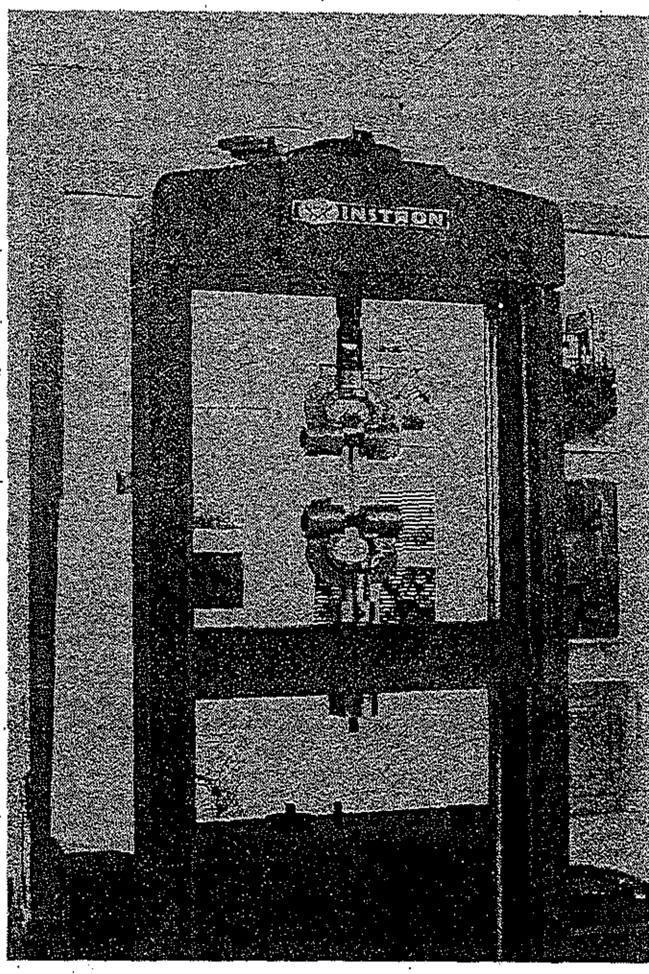

FIGURE A-1. - Instron TM 100-kg universal testing machine with test specimen.

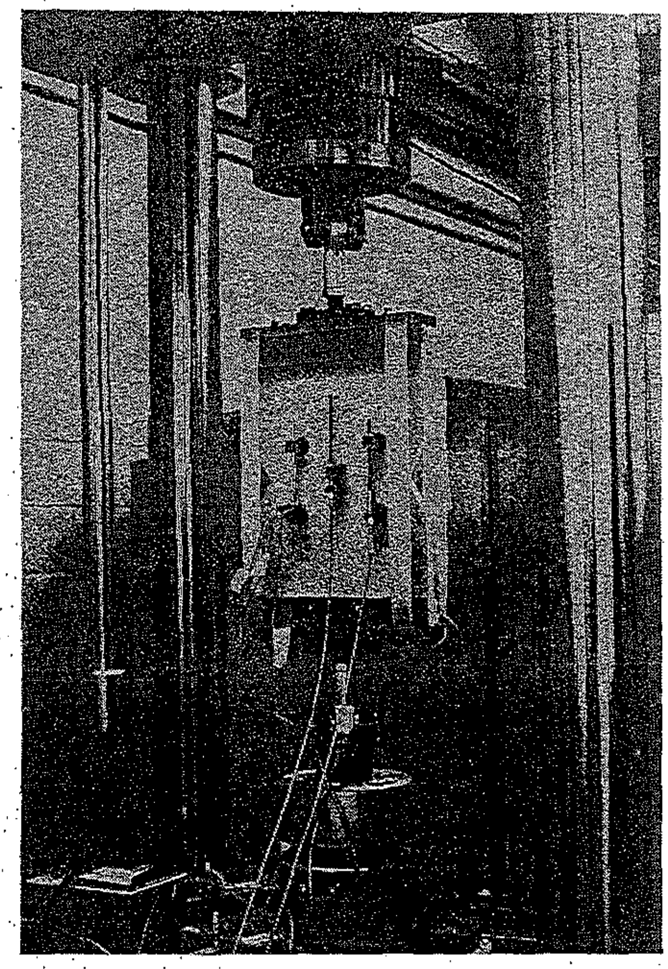

FIGURE A-2. - MTS 250-lbf electro-hydraulic loading frame with test specimen.

TABLE A-2. - Effect of gauge length on wallboard strain measurement

Location[1]	Strain system	Effective length, mm	Cyclic strain,[2] µin/in		
			Initial	After 4.45 h	Increased load
A........	Gauge.	3.18	80	82	470
B........	..do..	124	50	65	58
C........	Leaf..	[3]78	77	86	105
D........	Gauge.	3.18	69	69	320
E........	..do..	3.18	50	45	340

[1]See figure A-3.
[2]Cycled at 3.5 Hz.
[3]Center-to-center distance between posts.

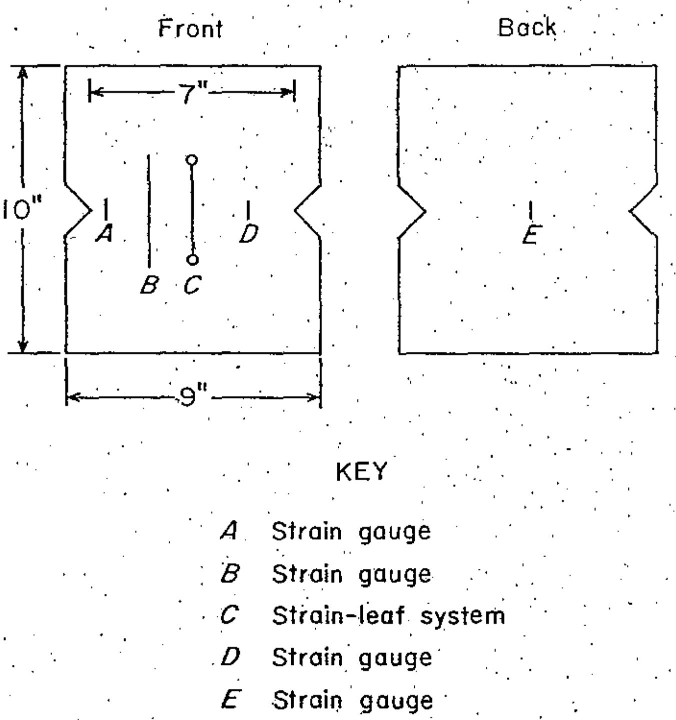

FIGURE A-3. - Wallboard test specimen and strain instrumentation.

The yield point and ultimate paper failure data at varying strain rates are listed in table A-3. The loading frame load versus deformation data for tests with different paper orientations are presented in figure A-5. Typically, the yield point, point *A* in figure A-5, was assumed to be the point of initial core failure; point *B* represents ultimate paper failure. For a given sample, when output from the strain measuring systems (table A-4) and their corresponding load-deformation curves (fig. A-6) are compared, discrepancies arise. Analysis of the readings in table A-4 points out that--

- Core failure, point *A*° on the strain time histories (fig. A-6), occurs at ~ 300 to 400 µin/in and may not be visible on the load-deformation curve.

- The initial yield point at *A* in figures A-5 and A-6, often attributed to core failure, is actually the first yield point of paper, although visual (naked eye) buckling or cracking occurs slightly beyond this point.

- Strain rate and orientation (transverse versus longitudinal) appear to affect ultimate failure, point *B*, but the strain at point *A* is relatively constant, ~ 790 to 840 µin/in for notched samples (and 1,000 to 1,400 µin/in for unnotched samples, as shown in table A-3).

- Cracking was visually observed at strain levels slightly beyond the yield strain.

Paper is the controlling factor for visual cracking in wallboard, and therefore its failure characteristics were further examined. Filament and paper failure have been discussed by several authors (37-42). For filament and paper sheets, there is a question as to the variation of the total elongation at break caused by strain rate (43-45). As shown in table A-5, average failure strains can reach ~ 13,000 and 20,000 µin/in for longitudinal and transverse paper samples, respectively. But for longitudinal and transverse wallboard samples (table A-3), the initial yield point does not vary appreciably nor does the ultimate failure typically reach these magnitudes. Once the core cracks, the paper strain localizes across the crack, and further elongation is limited until a break occurs. The average load at failure of wallboard paper, from table A-5, agreed with the failure load for unnotched wallboard in tests; i.e., 89 lb/in (longitudinal direction) × 2 (for both sides) is approximately equal to the average of the load-per-width values in table A-3, 176 lb/in, and values reported by the U.S. Gypsum Co. (table A-1). However, the transverse load test data did not agree; i.e., 2 × 20.7 lb/in for paper as compared to 58 lb/in for wallboard (table A-3) versus 80 lb/in (U.S. Gypsum, also for wallboard). Sample preparation alone could account for the variation (26).

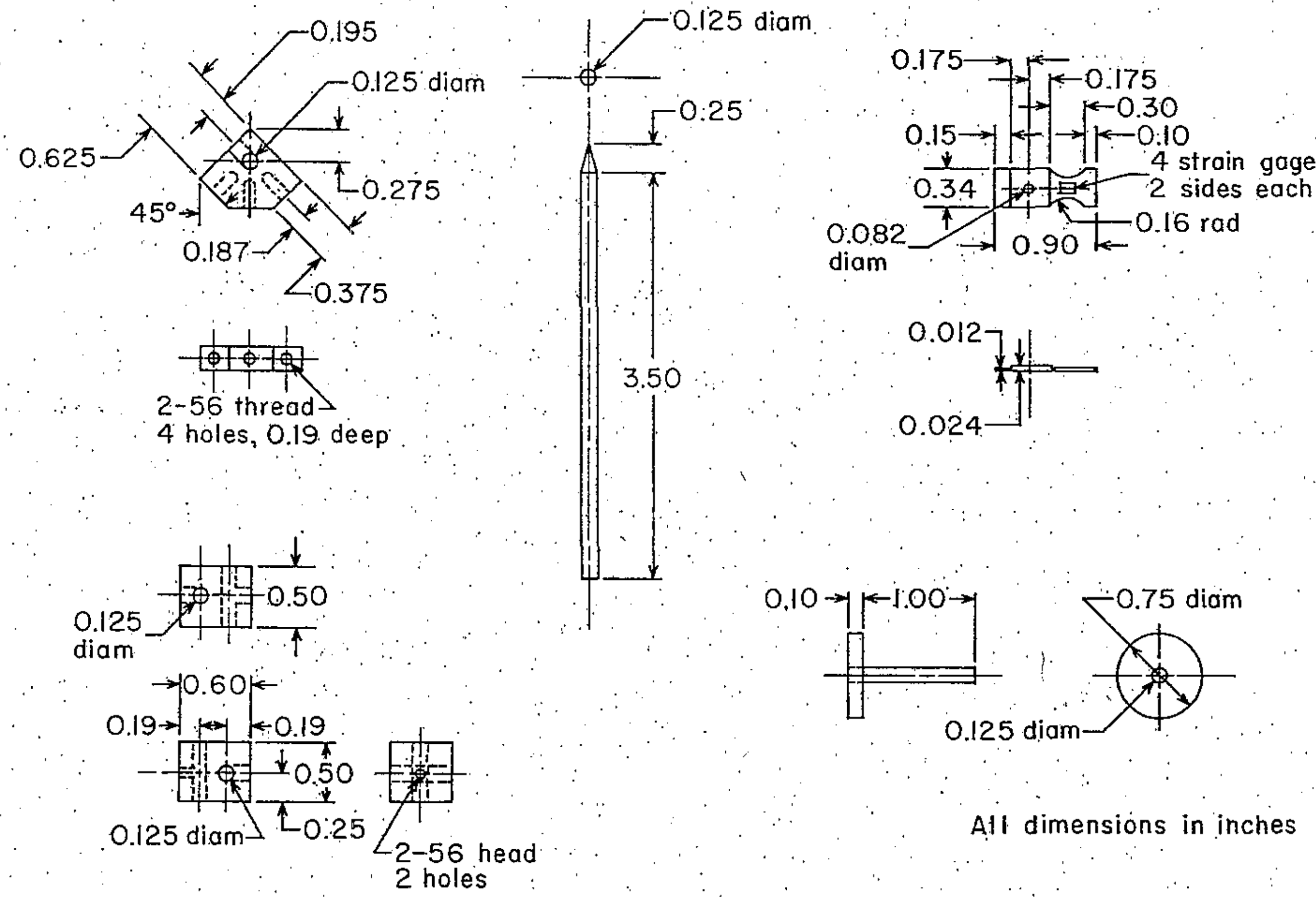

FIGURE A-4. - Details of post-mounted strain system.

Fatigue assessment was limited to a cursory look at the hardboard data presented in table A-1 and a limited fatigue test. Table A-2 displays the results for cyclic tests of wallboard under displacement control. As cyclic strain data were sought, strain systems were balanced to zero out baseline shift due to system drift and paper creep. Absolute displacement was not available. Load control was then utilized. Figure A-7 shows a wallboard test specimen, and the test results are listed in table A-6. System response on load control limited strain output to about 50 µin/in at an upper frequency of 2 Hz. The test was stopped at 66 h, after 475,000 cycles. Since the apparatus limited further tests, hardboard creep and fatigue data are presented, in table A-1, as a generalization of the response of wood products to cyclic and long term loads (10). Load versus number of cycles to failure (fatigue) is plotted in figure A-8, and load versus

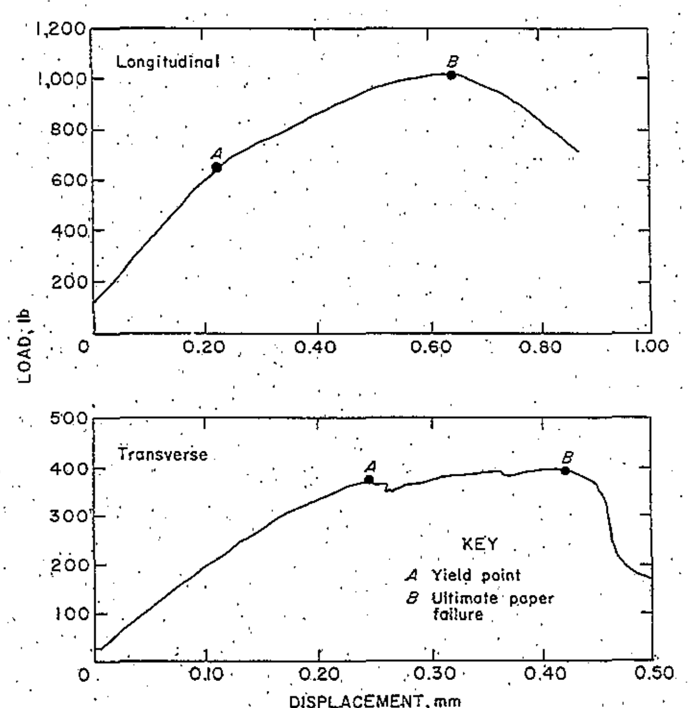

FIGURE A-5. - Effect of paper orientation on tensile failure curves for 1/2-in-thick wallboard.

TABLE A-3. - Results of laboratory tensile failure tests on 1/2-in-thick wallboard

Specimen	Length, in	Width, in	Yield point[1] Load, lb	Yield point[1] Strain, µin/in	Ultimate failure Load, lb	Ultimate failure Strain, µin/in	Ultimate failure Load lb/in width	Load rate, in/s	Time to failure, s
Longitudinal:									
With notch.....	10	6	528	1,180	703	3,770	117	0.000079	480
	10	7	585	945	899	2,700	128	.00157	17
	10	7	618	787	956	2,460	137	.0157	1.6
Without notch..	10	9	NA	NA	1,800	11,560	180	.00984	12
	10	9	618	1,260	NA	NA	NA	NA	NA
	10	9	607	1,420	NA	NA	NA	NA	NA
	16	9	618	1,076	1,550	8,860	172	.00984	14
Transverse:									
With notch.....	10	7	360	906	365	1,540	52.1	.00394	4.0
	10	7	332	866	371	1,810	53.0	.00394	14.6
	10	7	NA	NA	332	1,420	45.7	.197	.072
	10	7	NA	NA	410	925	59.0	.197	.047
	10	7	349	846	380	1,610	54.0	.00394	4.3
	10	7	354	935	377	1,620	53.4	.000787	21
Without notch..	10	9	512	1,100	490	1,540	56.9	.00394	3.9
	10	9	512	1,100	490	1,540	56.9	.00394	3.9
	10	9	517	1,160	540	1,500	60.0	.00394	3.8

NA Not available.
[1]Nonlinear response point of load-deformation curve.

TABLE A-4. - Comparison of strain readings from wallboard test specimen and from loading frame

Gauge location[1]	Measuring system	Effective gauge length, mm	Strain, µin/in [2]Point A°	Strain, µin/in [2]Point A	Strain, µin/in [2]Point B
Loading frame......	LVDT............	0.254	NA	787	2,460
1.................	Strain leaf.....	[3]77.85	352	724	NA
2.................	Kaman..........	[3]51.2	376	839	NA
3.................	Strain gauge....	12.7	334	817	NA

NA Not available.
[1]See figure A-6, diagram of test specimen.
[2]See figure A-6, plots of strain responses.
[3]Center-to-center distance between mounting posts.

TABLE A-5. - Results of tensile failure tests on wallboard paper

Sample group	Number of samples	Failure strain, µin/in	Load, lb/in	Time to failure, s	Sample group	Number of samples	Failure strain, µin/in	Load, lb/in	Time to failure, s
A(L)..	10	12,600	88	14.0	E(T)..	1	22,500	21	26.0
A(T)..	1	25,300	20	29.0	F(L)..	7	11,700	87	12.6
B(L)..	9	15,000	97	16.6	F(T)..	2	21,100	18.5	23.0
B(T)..	3	24,700	28	28.3	G(L)..	9	13,200	90	14.5
C(L)..	12	11,900	87	13.4	G(T)..	1	21,900	18	25.3
D(L)..	5	14,600	92	13.7	H(L)..	7	12,600	81	13.8
D(T)..	8	22,900	20	26.1	H(T)..	5	20,800	19	23.6
E(L)..	7	13,300	90	13.8					

(L) Longitudinal. (T) Transverse.

TABLE A-6. - Results of cyclic load tests on 1/2-in-thick wallboard

Location[1]	Strain system	Effective gauge length, mm	Cyclic strain,[2] µin/in			
			Initial	After 18.5 h	After 45.5 h	After 66 h
A.........	Gauge...	12.7	42	39	40	41
B.........	...do...	12.7	51	50	51	51
C.........	Leaf....	[3]76.35	64	64	66	65
D.........	Kaman...	[3]19.75	53	53	53	53
E.........	...do...	76.70	55	53	NA	56

NA Not available.
[1]See figure A-7.
[2]Cycled at 2 Hz.
[3]Center-to-center distance between mounting posts.

time to failure (creep) is plotted in figure A-9. Also plotted on the creep curve (fig. A-9) is the number of cycles to failure (from figure A-8) converted to time. The ratio of creep stress to fatigue stress appears to be independent of the time to failure and is ~ 1.5, lending itself to static design. Under repeated cyclic loading, the failure stress will be 0.67 times (~ 70 pct) that of static loading. By analyzing envelope data obtained at the test house, it was found that a ground vibration level of 1.0 in/s would induce a strain of ~ 100 µin/in in wallboard. This is only 10 pct of the strain required for failure, meaning that a large prestrain is needed to attain the cyclic failure stress level. Cyclic environmental factors are therefore the major strain producer, not blasting. Several assumptions were made in pointing out that blasting does not cause fatigue failure; however, the paper fatigue tests did point out that a large number of cycles are required to produce failure. Figure A-10 shows Wiss' measurements on gypsum wallboard (35) during an interlude in a program to deliberately induce cracking by blasting. Daily environmental cycles induced opening and closing of cracks of up to 0.1 mm. Wiss found the cyclic widening and closing of cracks to be unaffected by blasting activity.

Masonry Walls

The response of masonry walls to shear, flexure, and/or compressive loads has been studied by others (46-55). These investigators have indicated that the strength of a masonry wall depends on the mode of failure, compressive load, length-to-height ratio, amount of reinforcement, bond strength, rate of loading, grouting, and quality of workmanship. Workmanship alone can affect the wall strength by 60 to 80 pct (56).

The definition of cracks in brick and block walls is being debated. Cranston (32), Green (33), and Wroth (34) note that all brick and block walls have small 0.1-mm cracks upon completion. Green stated that 0.1-mm cracks are difficult to see and "therefore do not cause concern." Up to load failure, elastic approximation of the global deformation response appears reasonable (55). However, after cracking at local sites, the material is no longer a continuum, and the theory of elasticity does not apply. In lieu of using strain, a crack-width criteria has been proposed for cosmetic cracks that do not affect load-carrying capacity (33). However, the acceptability of crack widths varies with material. For concrete, 0.25 mm is the limit of acceptability (57), while 1 mm is the limit of acceptability for brickwork (34). The acceptability of crack widths also depends on who is making the judgment of acceptability; the public will generally accept cracks up to 0.2 mm wide in concrete, but the limit for engineers is 0.25 mm (57).

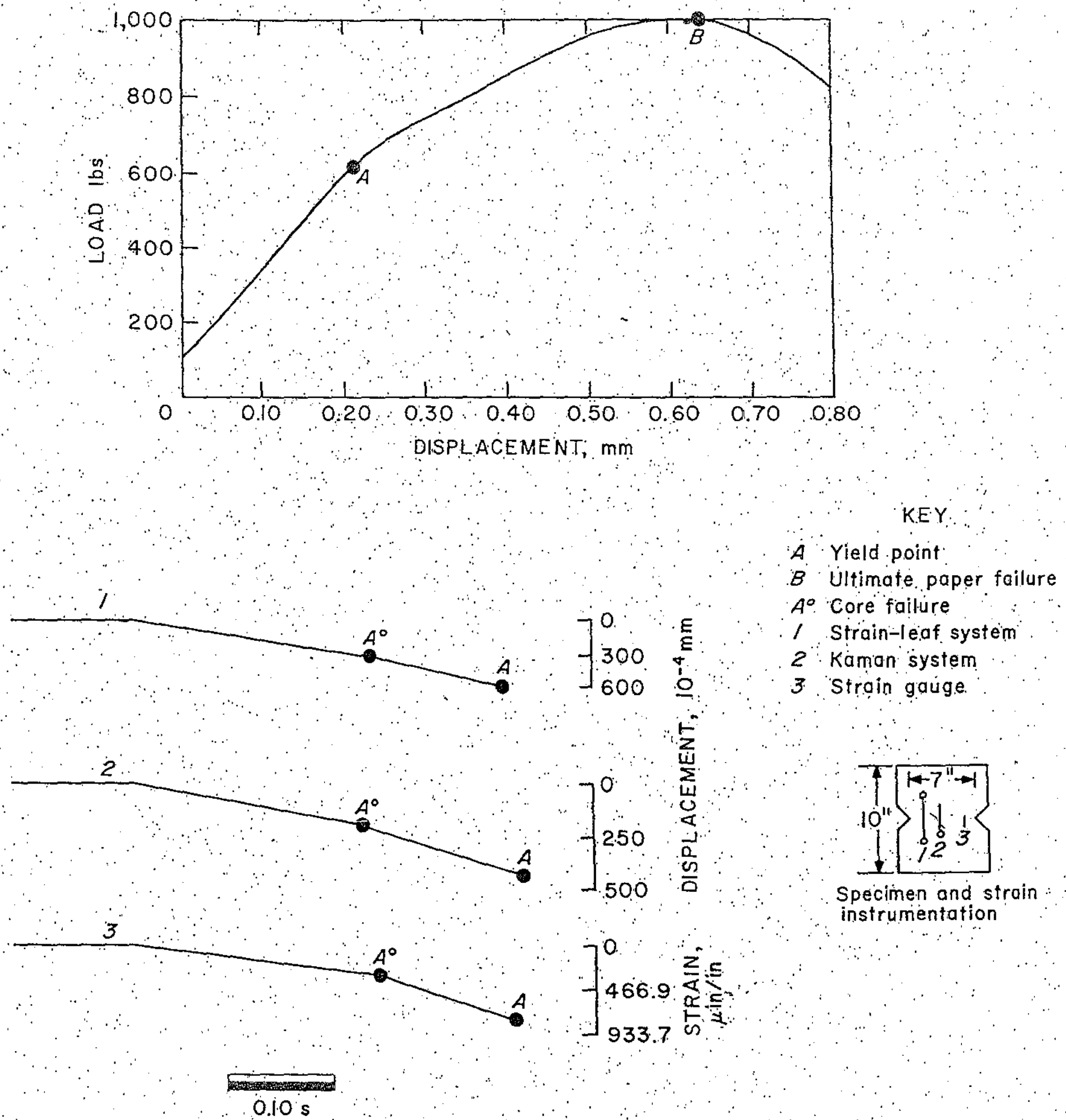

FIGURE A-6. - Comparison of tensile failure displacement data for 1/2-in-thick wallboard.

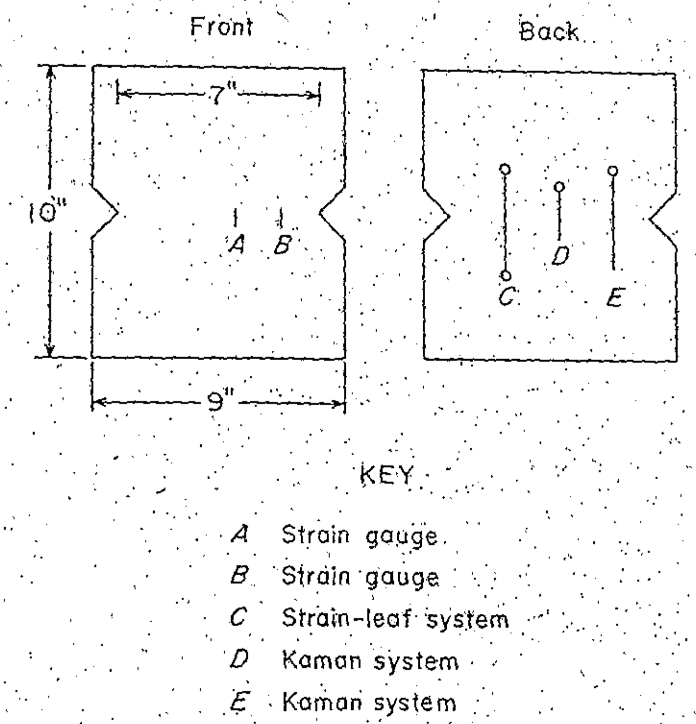

FIGURE A-7. - Wallboard specimen and strain systems tested under load control.

Masonry block and brick wall failure data from several sources are presented in table A-7, for both blasting- and laboratory-induced failure. A wide range of strain values is evident from these data. Variations were caused by use of different strain descriptors (global versus local strains) and strain gauges of different lengths. Crawford (31) reported dynamic strains of 300 µin/in across block mortar joints and 30 µin/in on the block at failure; but the author, correcting for gauge length, calculated a dynamic strain of 3,270 µin/in across the joints at failure. The calculated value was based on the assumption that the differential displacement occurs at the mortar joint-block interface, not uniformly over the entire 6-in strain gauge length. Using a joint width of 0.5 in, the 300-µin/in reading was adjusted by subtracting the 5.5 in of ~ 30 µin/in strain, converting to true displacement by multiplying by the 6-in gauge length, and then calculating strain by dividing by the 0.5-in joint width, i.e.,

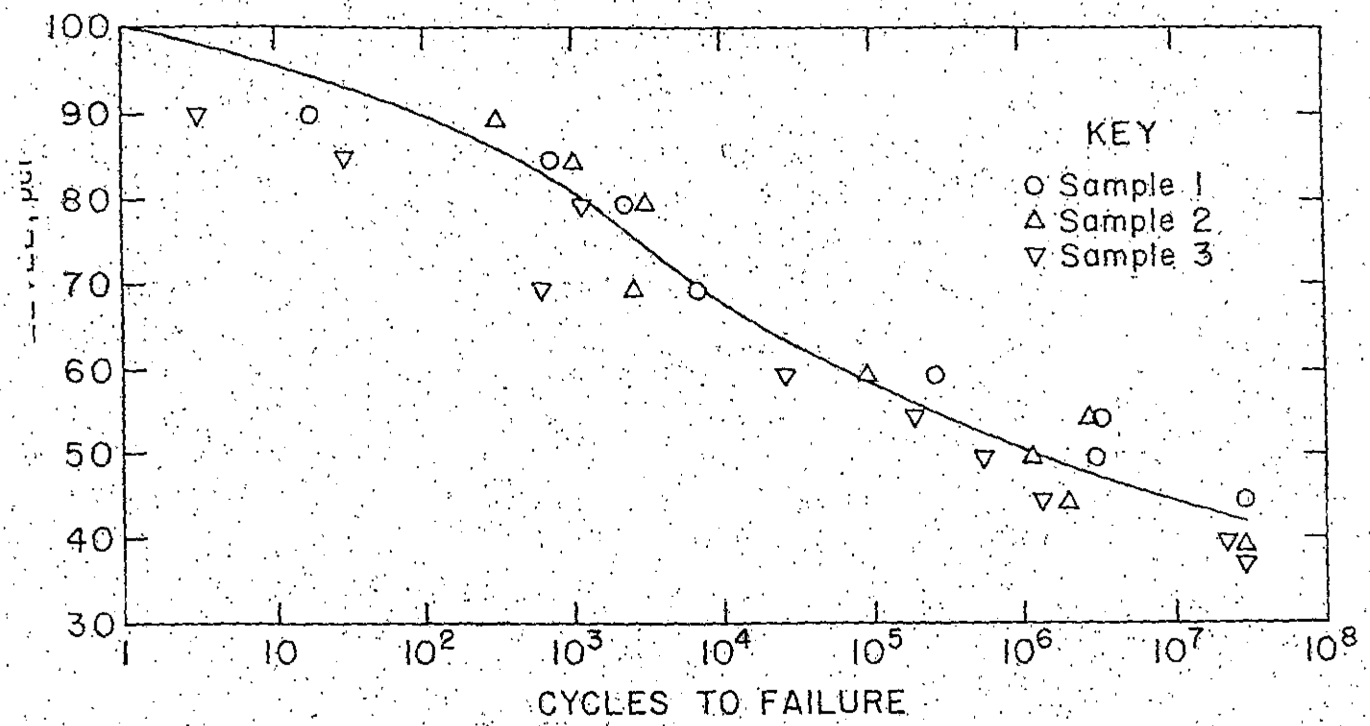

FIGURE A-8. - Stress level versus number of cycles to failure for 1/4-in-thick hardboard in tension (10).

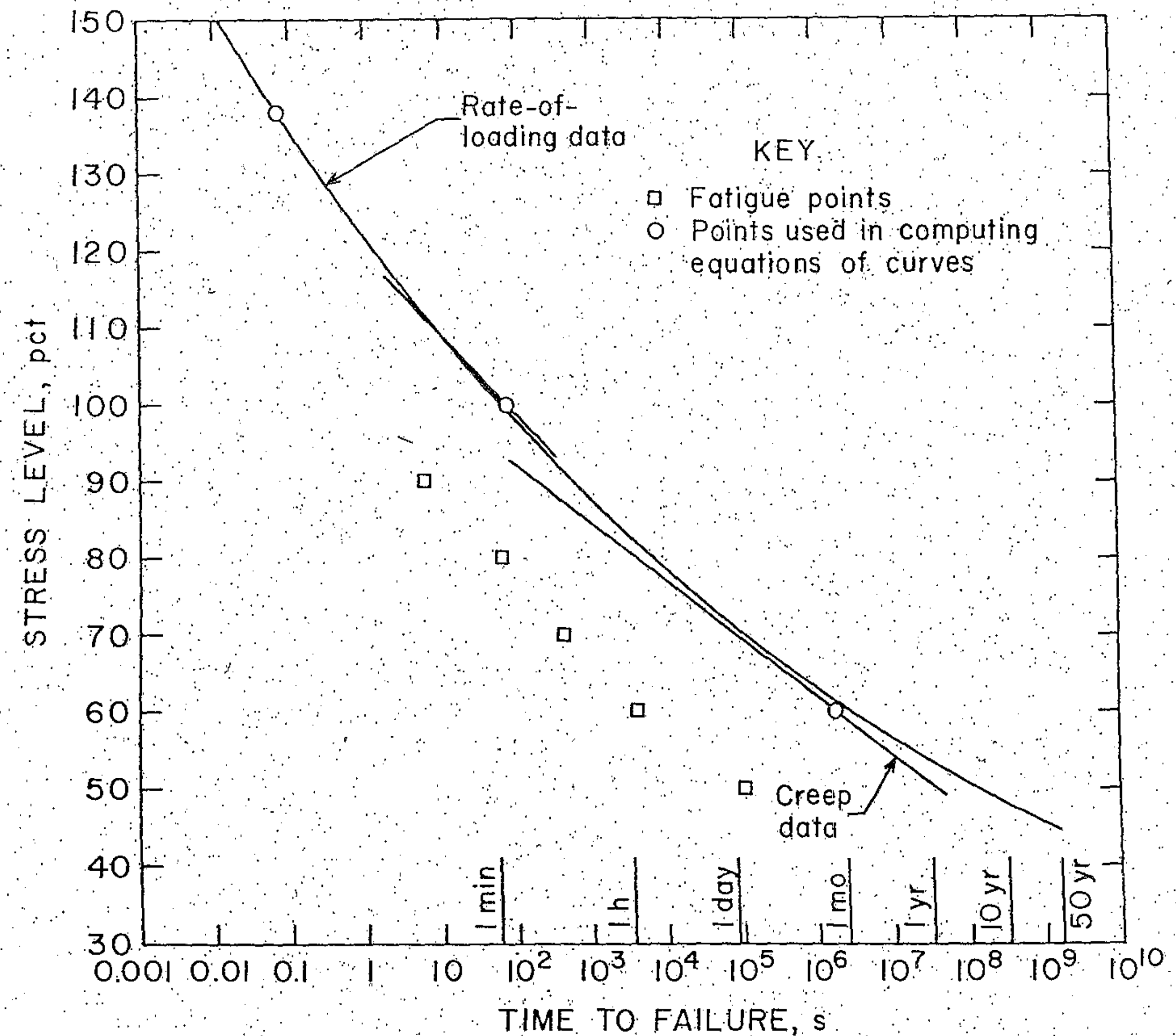

FIGURE A-9. - Stress level versus time to failure for 1/4-in-thick hardboard (10).

$$\frac{(300\ \mu in/in - 30\ \mu in/in \times 5.5 \div 6)\ 6\ in}{0.5\ in}$$

The uniformity of strain readings at joints throughout the wall and the relationship to global strain was studied in tests conducted under contract at the National Bureau of Standards (NBS) Tri-Directional Test Facility.

Fatigue Testing of Masonry Walls

NBS (Structure Division, Center for Building Technology) carried out the fatigue testing of masonry block walls. A synopsis of this investigation follows. Woodward (11), in an NBS report, discusses this contract investigation in greater detail. The investigators studied load-deformation response up to first cracking and nonlinear response during crack width growth. Additionally, fatigue effects were examined because previous research results (7-9, 46-56, 60) were limited.

Tests were run on ten planar 64- by 64-in walls (fig. A-11) and five angle walls 64 in high with 48-in-long legs

TABLE A-7. - Failure characteristics of block and brick walls

Investigator and type of material	Dynamic strain, µin/in	Strain gauge length	Longitudinal particle velocity, in/s	Type of cracking	Mode of deformation
Edwards (58), stone and mortar basement walls 18 to 24 in thick	[1]155, [2]300	NAp[3]	2.0	None	Predominantly flexure.
	[1]150, [2]150	NAp[3]	4.8	...do	Do.
	[1]375, [2]1,000	NAp[3]	10.6	Minor	Do.
	[1]450, [2]650	NAp[3]	10.0	...do	Do.
Northwood (59), stone and mortar walls (perpendicular to shot)	40	6 in	3.4	None	Do.
	45	6 in	4.5	Threshold	Do.
	45	6 in	7	Minor	Do.
	80	6 in	10	Major	Do.
Crawford (30):					
8- and 10-in concrete block	30	6 in	3	None	Do.
8- and 10-in concrete block mortar joints	300	6 in	3	Threshold	Do.
	[4]3,270	13 mm	3	...do	Do.
7- and 9-in poured concrete	100	6 in	10	...do	Do.
Mayes (9), 8-in hollow block piers (aspect ratio 2)	>500	NAp[5]	NAp	...do	Shear.
Hildalgo (7):					
8-in hollow block piers (fully grouted; aspect ratio 0.5; with vertical rebar)	>600	NAp[5]	NAp	...do	Do.
4-in brick (fully grouted; aspect ratio 0.5)	>800	NAp[5]	NAp	...do	Do.
Yokel (10):					
8-in hollow block wall, high-bond mortar	>110	NAp[5]	NAp	...do	Flexure; without compressive load.
4-in brick wall:					
Type A, 1:1:4 mortar	>160	NAp[5]	NAp	...do	Do.
Type A, high-bond mortar	>160	NAp[5]	NAp	...do	Do.
Type S, high-bond mortar	>160	NAp[5]	NAp	...do	Do.
Type B, high-bond mortar	>210	NAp[5]	NAp	...do	Do.
8-in hollow block, 4-in type-B brick, 1:3 mortar (composite wall)	>160	NAp[5]	NAp	...do	Do.

NAp Not applicable.

[1]Wall longitudinal to blast.

[2]Wall transverse to blast.

[3]Global strain measured by gauges mounted on steel straps fastened diagonally across walls.

[4]Calculated value of strain deformation occurring in 13-mm-wide mortar joint.

[5]Global strain computed from LVDT displacement measurements at corners and midwalls when cracking was observed.

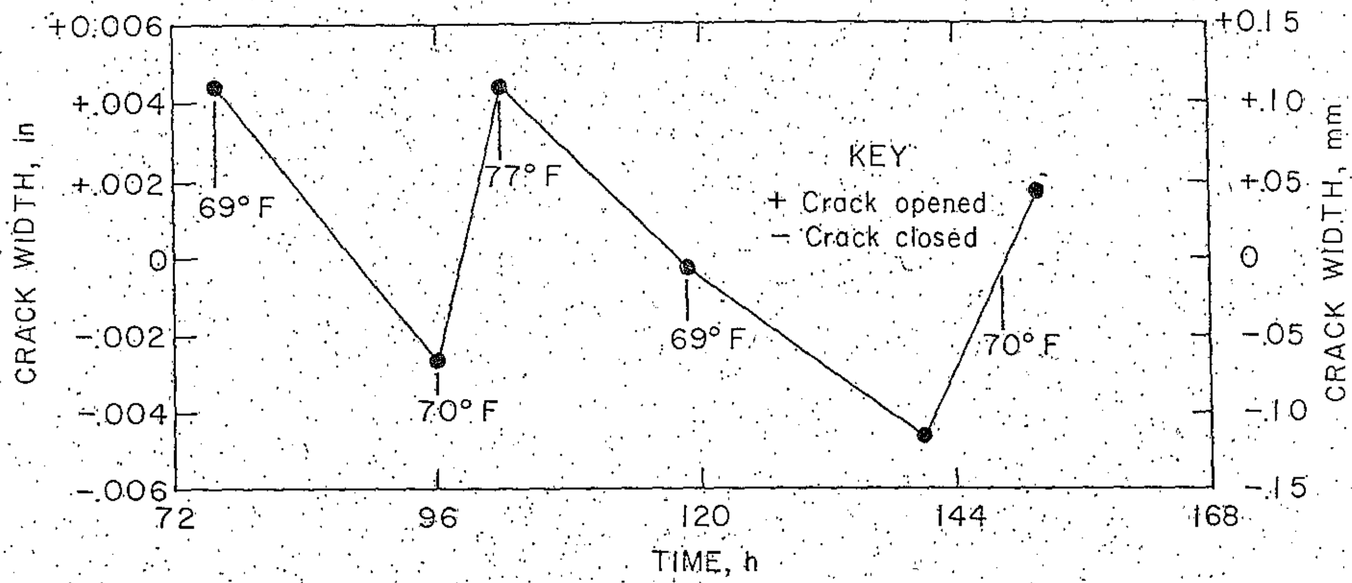

FIGURE A-10. - Response of wallboard during a period of nonblasting (35).

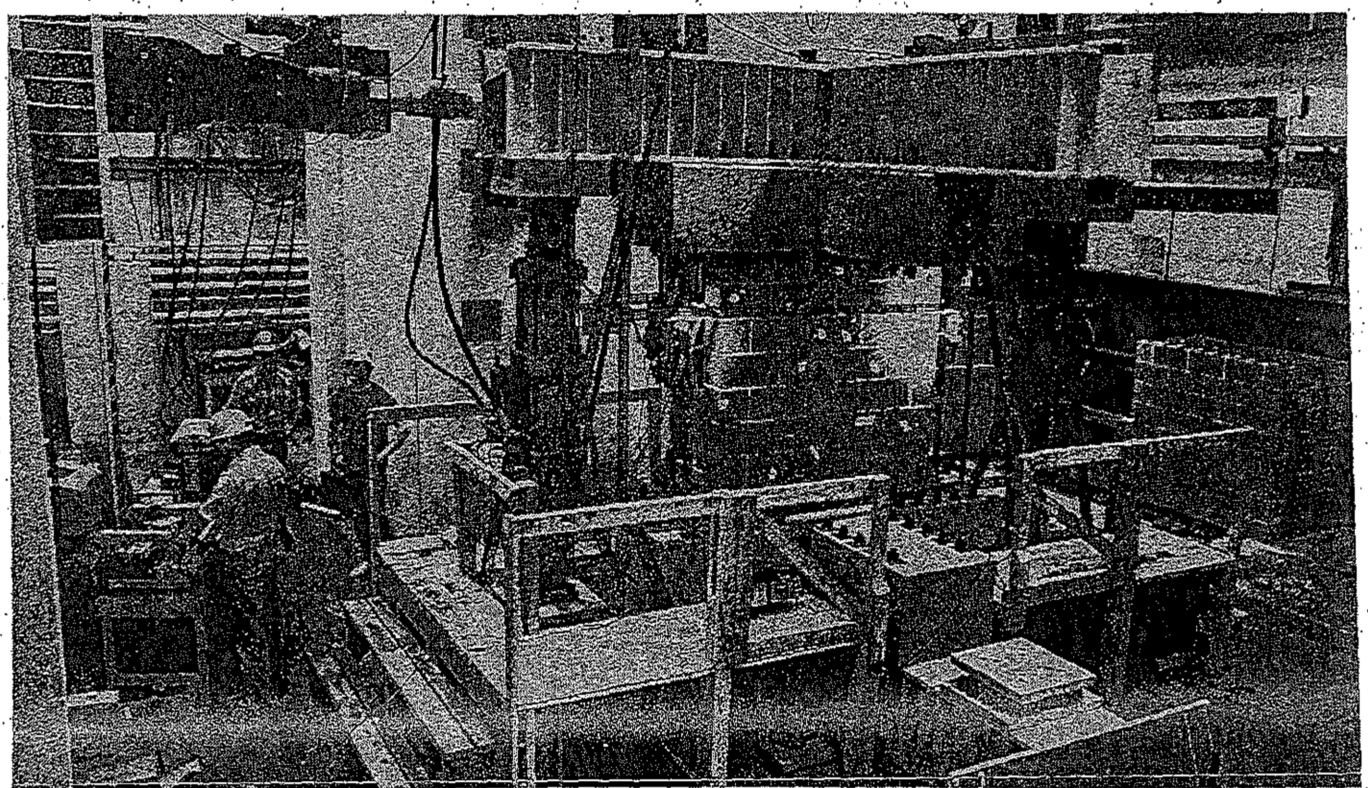

FIGURE A-11. - In-place 5- by 5-ft masonry block wall at NBS Tridirectional Test Facility.

(fig. A-12). Both figures show an epoxied in-place wall. Walls were laid in running bond,[1] and standard ASTM tests were run on mortar (mortar type N) and prisms (3 blocks stacked vertically). All walls were manufactured 30 days prior to testing.

[1]Blocks were laid overlapping 50 pct, with head joints in alternate courses in vertical alignment.

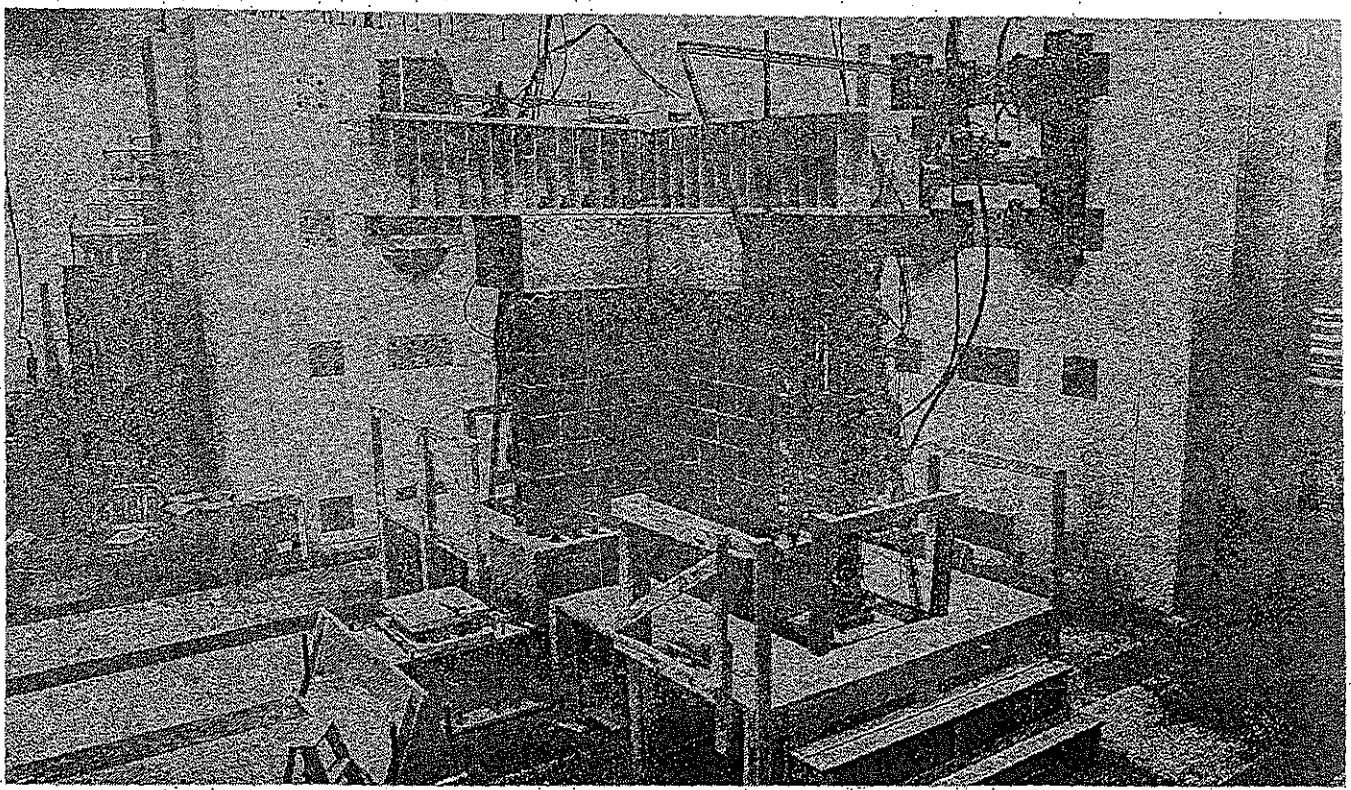

FIGURE A-12. - In-place angle wall with 4-ft-long legs at NBS Tridirectional Test Facility.

Strains were measured across the joints and assessed by LVDT global displacements of the wall. Voltage outputs from the Bureau of Mines strain systems were digitized by NBS for direct readouts of strain. Initial tests at 26 strain sites revealed that vertical gauges would not pick up any shear displacement. Consequently, only 15 gauges were needed for the remainder of the tests. These were primarily horizontal except for vertical gauges monitoring flexure stress and a gauge on the block. Figure A-13 shows a typical test sample, including the strain gauge locations, LVDT global displacement, and pretest crack locations. Pretest cracks were mapped to delineate the extent of shrinkage and workmanship cracking from one specimen to another. Cracking observed was similar in all walls, but the extent varied. Crack inspections were conducted at 1/2-h intervals or when major strain changes were observed. These midtest inspections required the aid of an eyepiece with a magnification of 7 X to easily distinguish cracks of 0.1 mm. Upon completion of the test, at ultimate failure, a map of the major cracking pattern was drawn.

The test program was varied to define under what conditions blasting could induce failure. Initially, global displacement and strain characteristics at cracking were assessed. Cyclic tests were then conducted, with and without prestrains, depending on previously observed failure displacements. Each test was used to define limiting conditions, and therefore few replicate in-plane shear tests were run. The tests were conducted as follows:

- The walls were epoxied in place to the upper and lower footing by lowering the upper crosshead on the bedded epoxy until a load of 500 to 1,500 lbf was sensed. The initial set took 1 h, and no tests were run until it had hardened at least 16 h. Loading was applied by the upper crosshead in the direction of the LVDT arrows in figures A-13 and A-14.

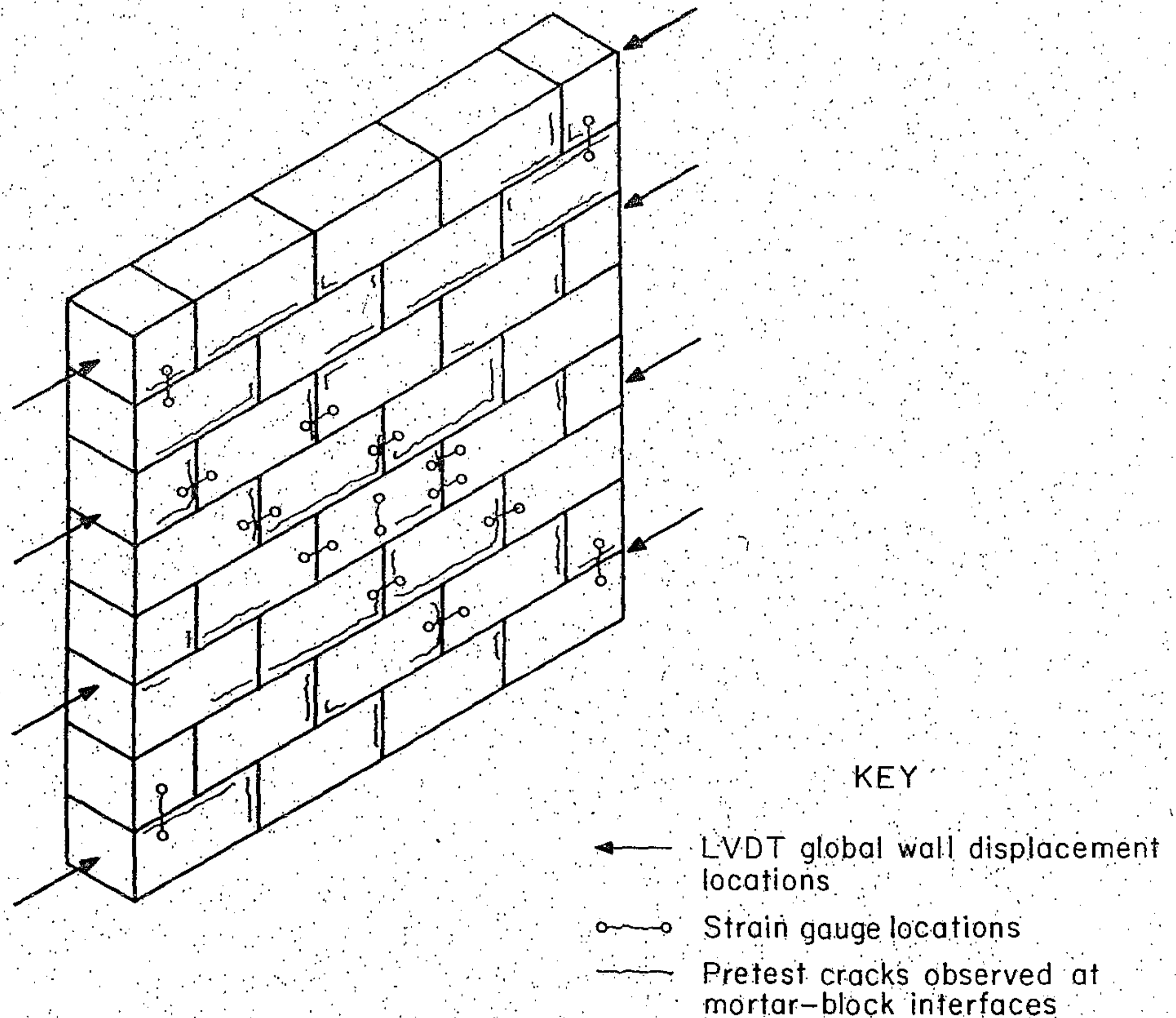

FIGURE A-13. - Typical LVDT global displacement and strain gauge locations with pretest crack observations.

- Monotonic or ramp loading was examined first to establish in-plane top-wall global displacements and cracking characteristics. Five tests of this type were run at various times to confirm results seen under cyclic loading but missed in previous tests.

- The effect of strain rate was assessed globally since the cyclic response of the system was limited to under 5 Hz for large cyclic displacements. The wall was displaced to up to one-half the failure level at rates equivalent to frequencies of 0.003 and 3 Hz. The test indicated that rate did not affect response. However, after testing was completed, it was observed that one wall did have a higher failure level when subjected to faster loading. As discussed in the next paragraph, this cyclic rate effect is believed to be small when considered for blasting, since frequencies of 6.5 Hz were achieved in cycling the wall that had the higher failure level.

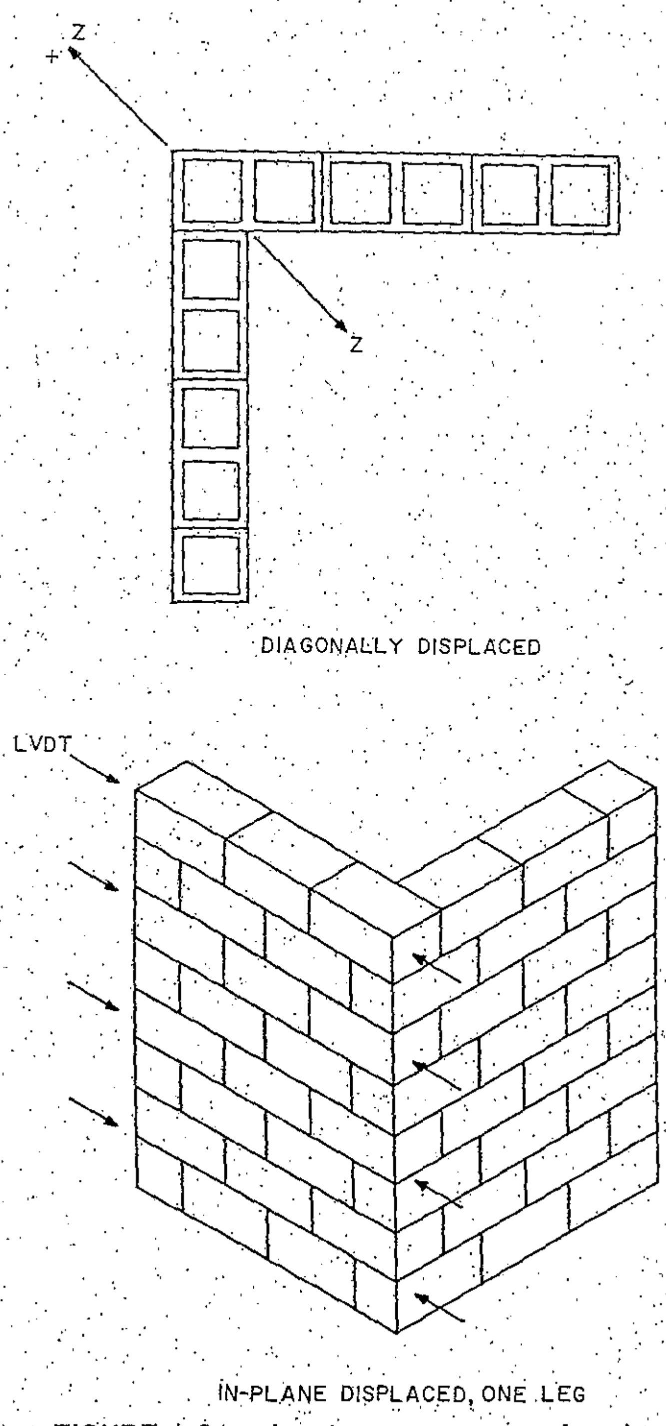

FIGURE A-14. - Loading orientations of angle wall along the diagonal and in-plane (one leg).

• Cyclic response started at 0.001 in global displacement, producing ±50 µin/in as measured at a local site, and continued for 100,000 cycles. Because of variations of strains at local sites, global displacements were used to control the tests. Global cyclic limits were set at 0.005 and 0.011 in. Due to time limitations and a lack of cracking, the amplitude was increased until a diagonal crack ~ 0.06 in wide occurred. Displacement levels were beyond those expected from blasting (i.e., assuming simple harmonic motion and that displacement only occurs at the upper corner of the basement wall, a 1.0-in/s ground motion gives a displacement of 0.024 in at 6.5 Hz).

• A prestrain was then added by displacing the wall from 0.002 to 0.044 in. Cycling resumed at ±0.003 in displacement for 100,000 cycles or to failure.

• Similar monotonic and cyclic tests were conducted on the angle walls. The first wall was failed monotonically along the diagonal (fig. A-14). The wall displayed failure displacement levels equal to the resultant of the inplane resistance of each leg. Consequently, remaining tests were conducted inplane along one leg (fig. A-14). The outstanding leg was found to have little effect on the in-plane leg's wall capacity or failure mode.

The observations of cracking and global versus local strain readings from these tests are described below.

Cracking

All cracks initially observed were at eye threshold limits, ranging in width from 0.01 to 0.1 mm. Even over limited wall areas, local cracking was hard to distinguish from existing shrinkage and workmanship cracks. Areas where strain readings were high allowed for threshold observation of local cracking. When strains reached ~ 700 µin/in, cracks ~ 0.01 mm wide could be observed with the aid of a 7-power magnifying eyepiece. Local cracks occurred randomly at mortar-block interfaces before the major failure crack appeared in each wall. These cracks, which ran diagonally along mortar-block interfaces from corner to corner of the wall, formed just prior to reaching the ultimate load capacity (maximum in-plane load) shown in table A-8. The diagonal steplike cracks were not affected by localized cracking and are

TABLE A-8. - Masonry wall test parameters (11)

Wall	Precompression axial load, lbf	Loading history and type	In-plane load, lbf[1]	Axial load,[2] lbf	In-plane displacement,[2] in	
					Ram	Wall
1..	14	Cyclic, prestrain	24.4	28.8	0.087	0.050
2..	14	Monotonic, ramps.	22.2	29.6	.226	.073
3..	14	Cyclic, prestrain	21.2	36.6	.135	.061
4..	14	...do............	27.0	35.9	.162	.106
5..	4	Cyclic, reversed.	17.5	16.9	.082	.053
6..	5	Monotonic, ramps.	27.3	33.0	.167	.129
7..	18	Cyclic, prestrain	30.0	37.2	.131	.087
8..	13	Cyclic, reversed.	19.4	21.8	.093	.063
9..	16	Cyclic, prestrain	23.2	54.1	.256	.136
10..	16	...do............	21.7	35.5	.138	.080
11..	16	Monotonic........	19.1	31.7	.129	.084
12..	16	...do............	17.6	30.6	.129	.084

[1]Maximum.
[2]At point of maximum in-plane load.

similar to the one observed in the southeast basement wall of the test house. However, a crack of this kind would not be generated in a house by in-plane shear alone because the large vertical compressive loads needed to produce this type of failure (>65 lb/in^2) are not present in a typical residential house.

Strains

Strains read at local sites showed an inflection point at ~ 100 µin/in, but visual cracking occurred anywhere from 500 to 1,000 µin/in. Allowing for variations in mortar thickness and strain gauge inaccuracies, this compares to the predicted visual threshold of 700 to 7,000 µin/in. Most of the strain occurred across joints, which had an assumed average width of 13 mm. Strains measured on the walls varied considerably from tension to compression. Therefore, readings had to be assessed over the entire wall to predict what diagonal path the major failure crack would follow. As it turned out, predicting the exact diagonal for final faiure was difficult, due to both loading history and overall differences in sample condition. There appeared to be a minimal global displacement or strain at which the major

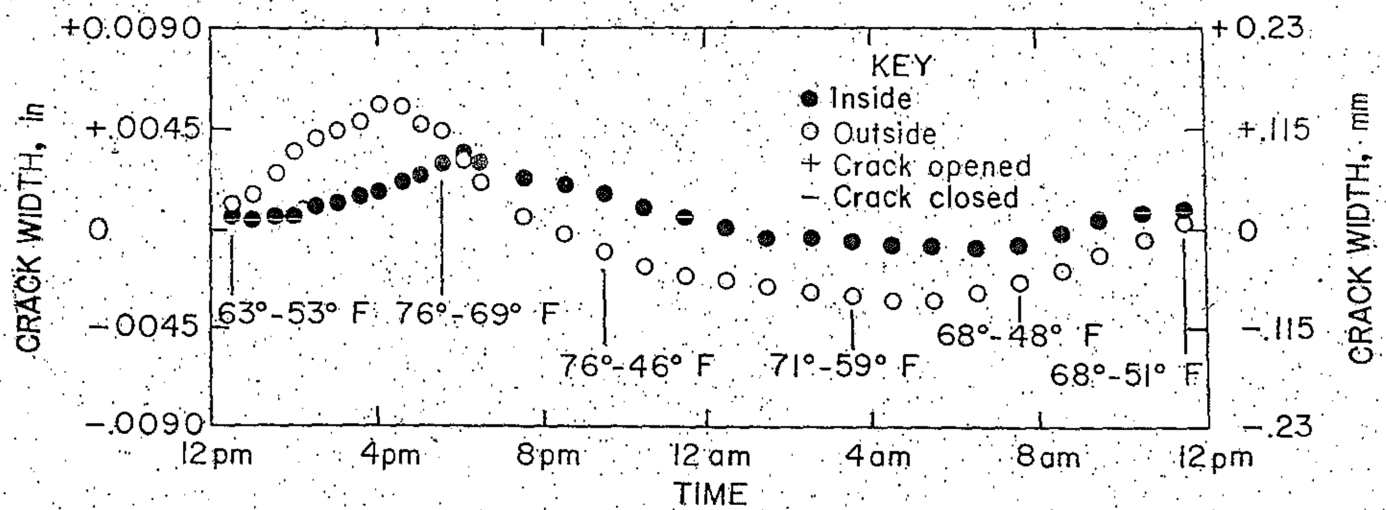

FIGURE A-15. - Response of concrete block crack widths to environmental factors (28).

diagonal crack occurred (~ 600 μin/in). Cycling at low global strains (50 to 100 μin/in) appeared not to affect the global failure strain necessary for cracking. Cycling at 50 to 100 μin/in about an offset displacement near the global failure level appeared to shift the absolute global failure strain to a higher value. While in-plane shear failure is not applicable for houses due to the high compressive loads it requires, the strain results are still valid. Research at NBS scheduled for fiscal 1984 will continue examination of masonry wall failure (61).

Widening of cracks in masonry joints has been discussed by others (28, 62). Figure A-15 shows Wall's (28) measurements of changes in crack width in concrete block walls with daily temperature variations in a desert environment. As in houses with wallboard, daily environmental cycling induced crack width changes of up to 0.1 mm. Long term changes in brickwork piers are affected by moisture, fluctuating temperatures, type of brick and mortar, and the presence of a dampproof course (63-64).

APPENDIX B.--DESIGN DETAILS OF TEST HOUSE

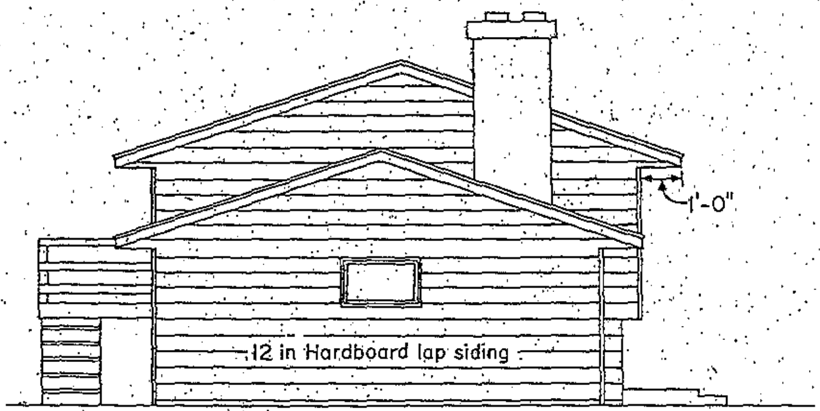

NORTH ELEVATION

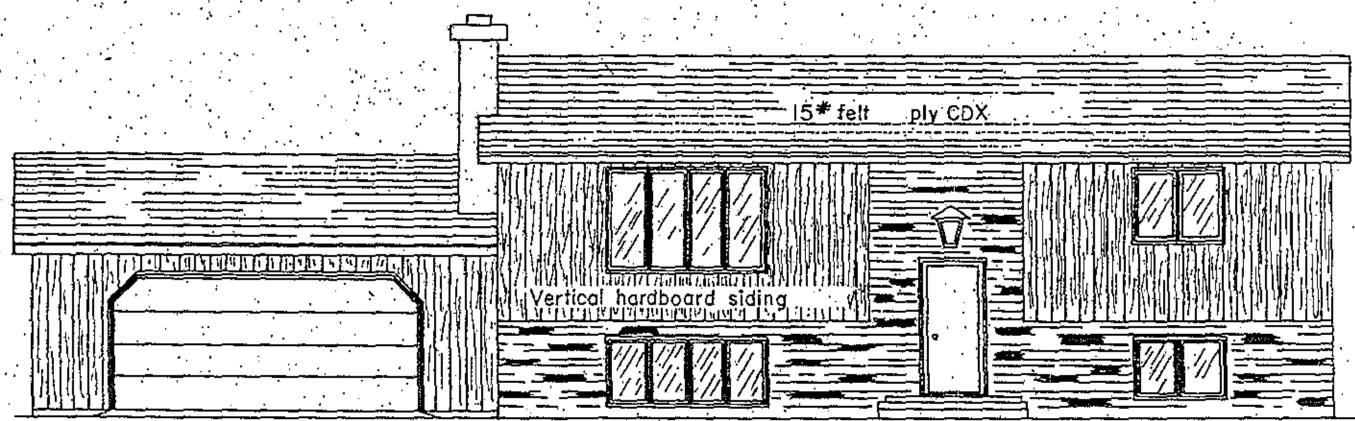

WEST ELEVATION

FIGURE B-1. - North and west side elevation views (architect's drawing).

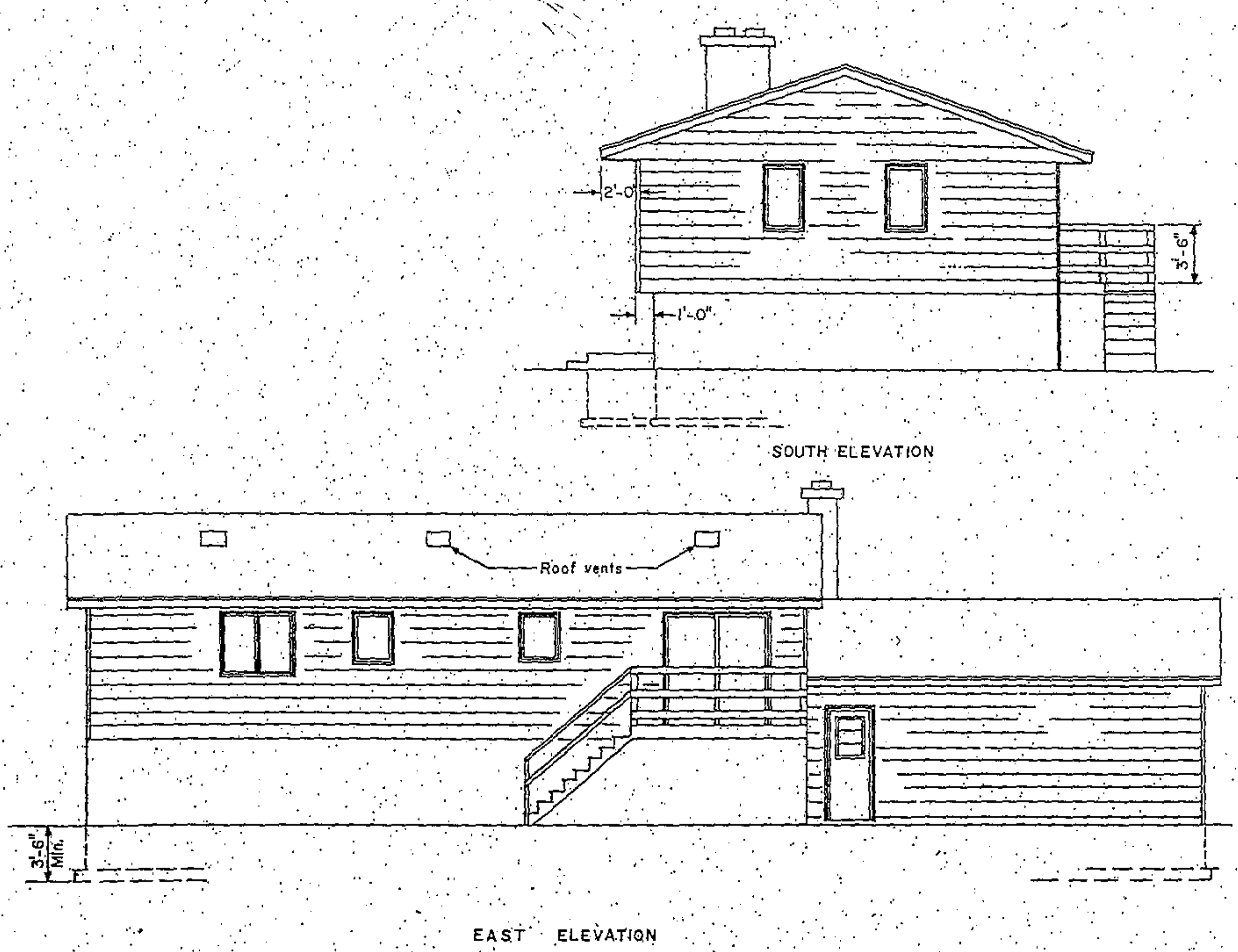

FIGURE B-2. - South and east side elevation views.

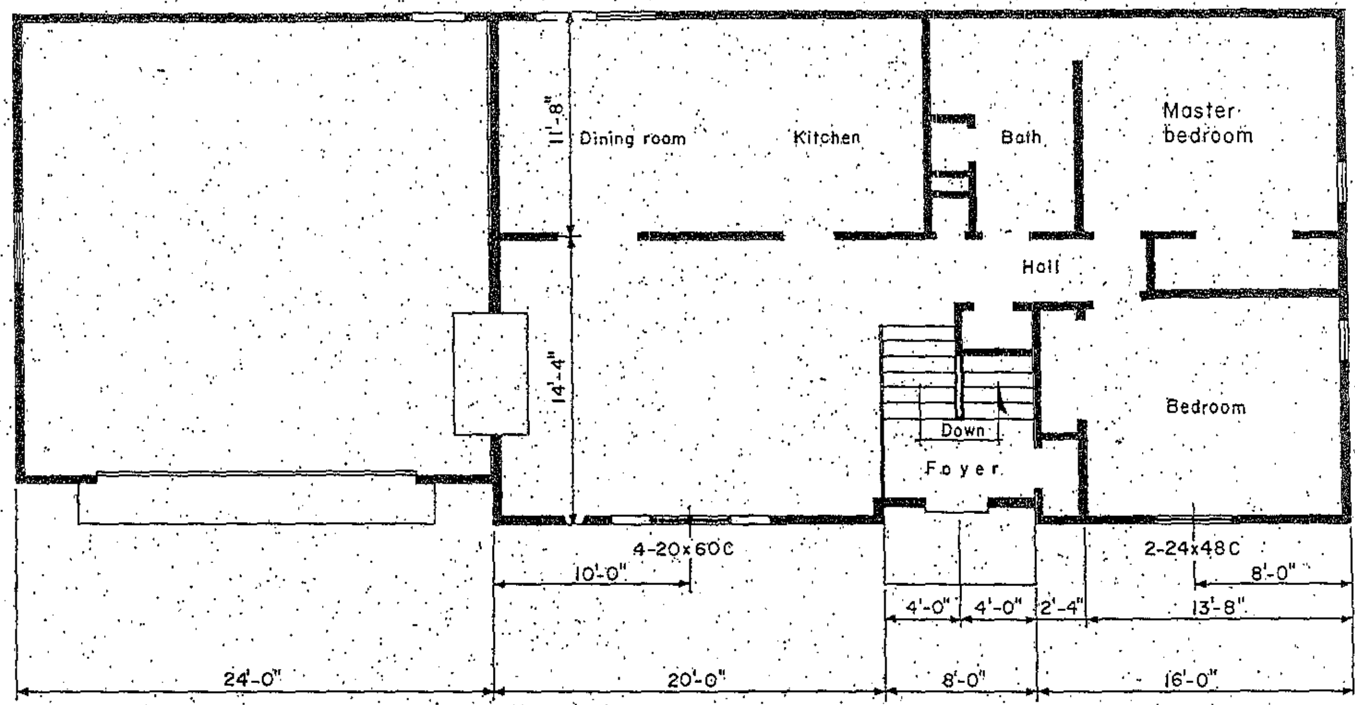

FIGURE B-3. - Main floor plan.

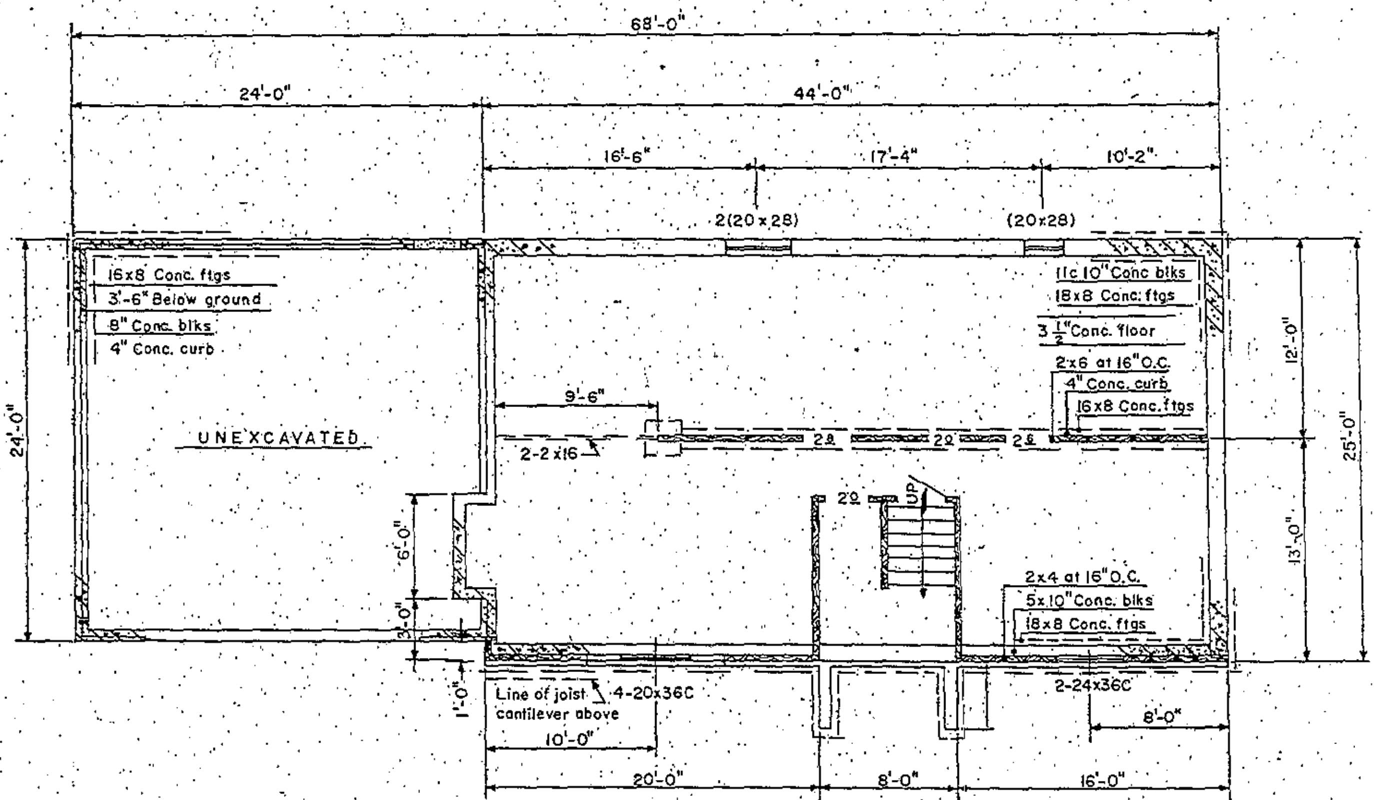

FIGURE B-4. - Basement floor plan.

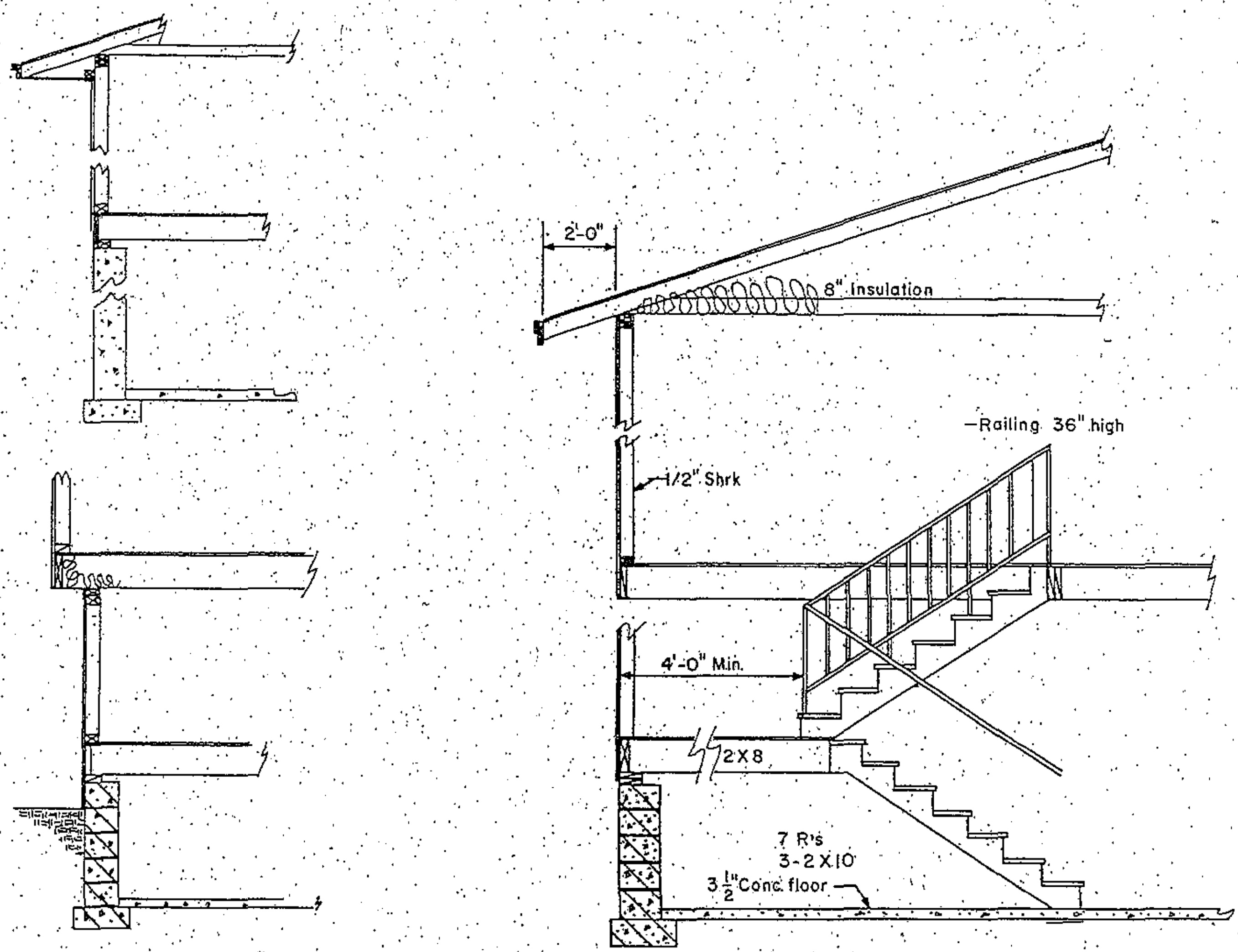

FIGURE B-5. - Design details.

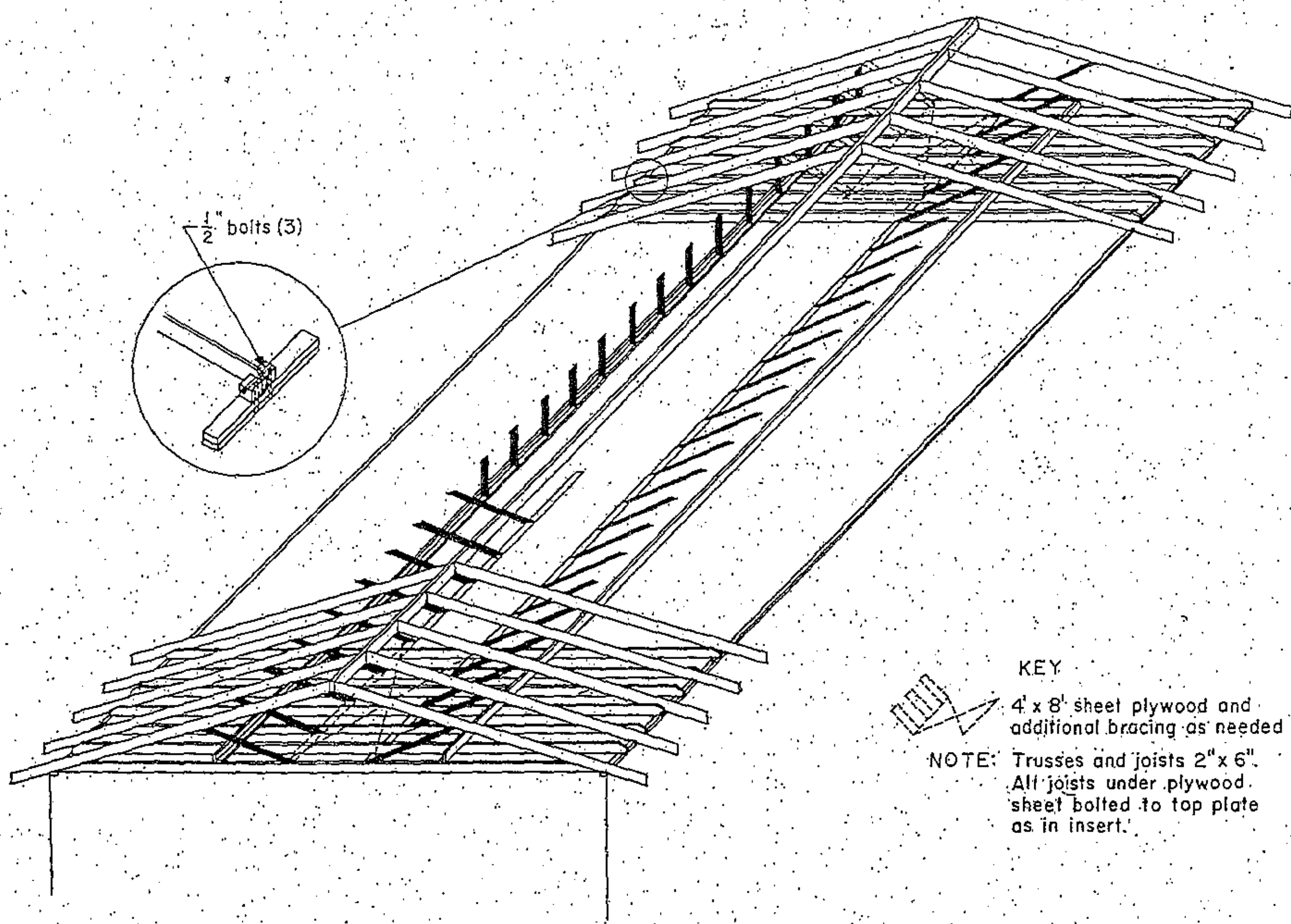

FIGURE B-6. - Roof framing after modifications.

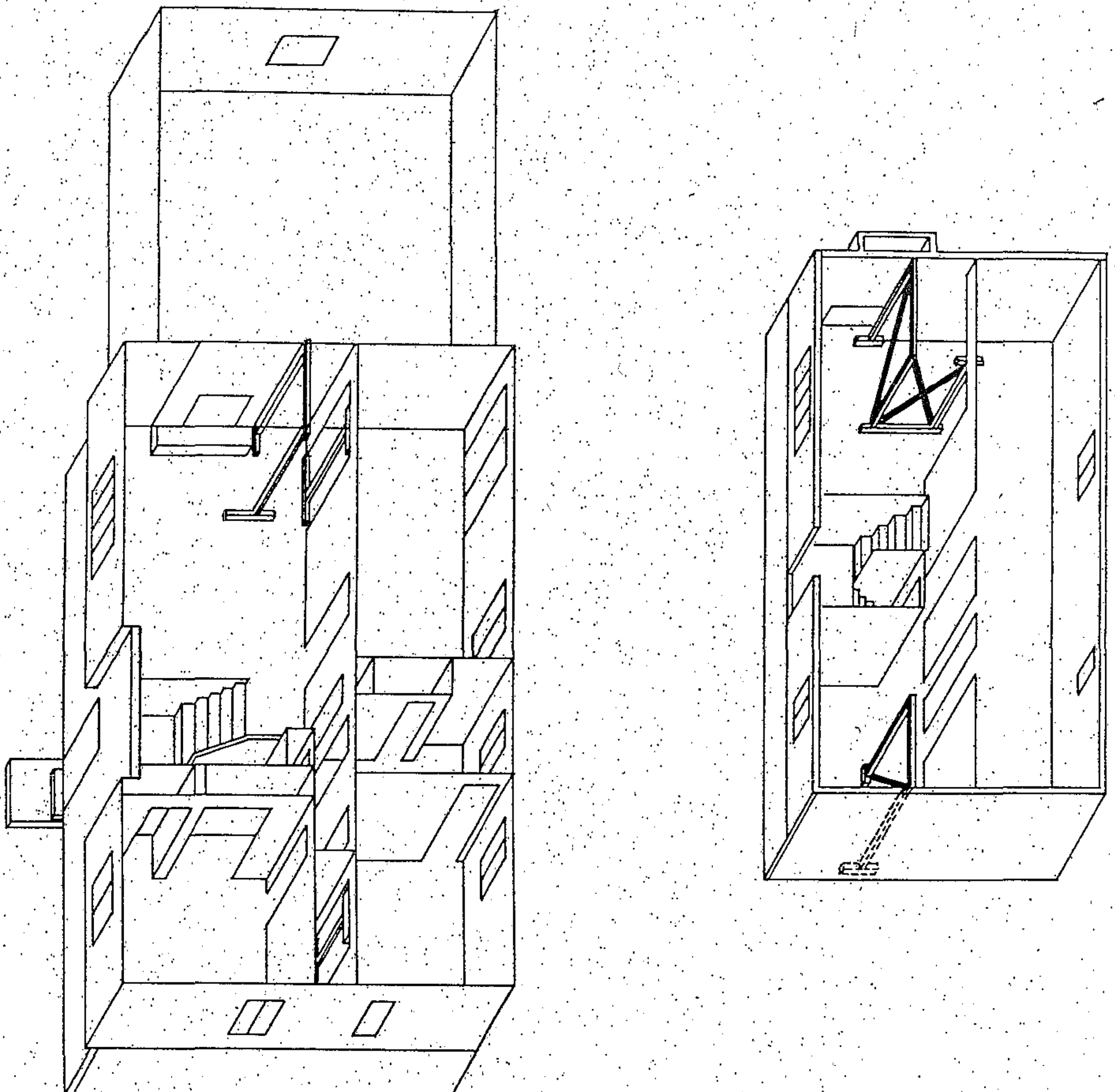

FIGURE B-7. - Structural modifications of main floor and basement to accept shakers. (Modifications shown as darkened features.)